Supporting Information

Multi-State Amine Sensing by Electron Transfers in a BODIPY Probe

Katherine L. VanDenburgh, Yun Liu, Tumpa Sadhukhan, Christopher R. Benson, Natalie M. Cox, Sundus Erbas-Cakmak, Bo Qiao, Xinfeng Gao, Maren Pink, Krishnan Raghavachari, and Amar H. Flood*

S1. Materials and Methods

All reagents were obtained from commercial suppliers and used as received. Column chromatography was performed on silica gel (160–200 mesh, SiliCycle Inc., Canada). Thin-layer chromatography (TLC) was performed on pre-coated silica gel plates (0.25 mm thick, SiliCycle Inc., Canada) and observed under UV light. Preparatory thin-layer chromatography (prep-TLC) was performed on hand-made silica-coated glass plates. The plates were prepared with 80 g of silica gel, 1.0 g of Plaster of Paris for adhesion, and 0.1 g of zinc orthosilicate (fluorescent indicator). These were suspended in 110 mL of deionized water, and carefully poured over a glass plate (20 × 20 cm^2) for an even coating. The plates were air dried for 12 hours before use. All high performance liquid chromatography (HPLC) purifications were on a reverse-phase, C18 column with a gradient of water and acetonitrile, buffered at 0.1% trifluoroacetic acid.

Nuclear magnetic resonance (NMR) spectra were recorded on Varian Inova (500 MHz, 400 MHz) and Varian VXR (400 MHz) spectrometers at room temperature (298 K). Chemical shifts were referenced to residual solvent peaks. High resolution electrospray ionization mass spectroscopy (HR-ESI-MS) was performed on a Thermo Electron Corporation MAT 95XP-Trap mass spectrometer. For the cationic BODIPY compounds (**BQuMe**•I and **BQuMe**•PF_6), the high resolution mass spectroscopy was reported in negative mode with two anions (either I^- or PF_6^-).

All spectroscopy experiments were performed with high purity organic solvents in a 1 × 1 cm quartz cuvette at room temperature (298 K). Electronic absorption spectra were measured on a Varian Cary 5000 UV-vis-NIR spectrophotometer. Fluorescence studies were performed on the following two instruments. The first was a Photon Technology International custom modular system consisting of a QuantaMaster^{TM}-40 and a LaserStrobe^{TM}. For steady-state measurements, a 75 Watt xenon arc lamp was used as the light source, and a photomultiplier tube (PMT) as the detector. The LaserStrobe^{TM} utilized a dye laser (Coumarin 500) pumped by a nitrogen source for the time-resolved spectroscopy. The second fluorimeter was an Edinburgh Instruments' FLS1000 Spectrofluorometer. The FLS1000 utilizes a 450 W Xenon lamp for excitation, and a Hamamatsu R13456 PMT for detection. Spectra are corrected for lamp intensity using a silicon reference detector, and the emission spectral response was corrected for intensity and wavelength from calibrated lamps. Time-correlated single photon counting (TCSPC) fluorescence lifetimes were recorded on the FLS1000 using an Edinburgh Instruments EPL/EPLED 450 nm laser, with a maximum signal of no more than 3% of the repetition rate to avoid pulse-pileup.

The fluorescence quantum yields of **BQu** and **BQuMe**$^+$ were determined by reference to rhodamine 6G[S1] and ruthenium(II) trisbypyridine dichloride[S2] respectively. Each quantum yield measurement was a variable concentration experiment, based on Equation S1.

$$\phi_x = \phi_{ST} * \frac{Grad_x}{Grad_{ST}} \frac{\eta_x^2}{\eta_{ST}^2} \qquad \text{Eq. S1}$$

where ϕ was the quantum yield, $Grad_x$ and $Grad_{ST}$ were the slope of a plot of the absorbance at the excitation wavelength versus the integration of the emission for the sample (x) and the standard (ST) respectively, and η was the viscosity of the solvent. For the quantum yield of **BQuMe**$^+$ in the presence of triethylamine, the absolute quantum yield was measured with an integrating sphere on the FLS1000. The experiment was replicated and the reported value was the resulting average and standard deviation.

Electrochemical experiments were conducted in a conical glass cell with a standard three-electrode setup for cyclic voltammetry (CV). The electrodes used were a 2 mm diameter glassy carbon working electrode, a platinum wire counter electrode, and a polished silver wire pseudoreference electrode. The metal electrodes were washed with distilled water and acetone prior to use. The working electrode was polished with an alumina paste prior to washing with distilled water and acetone. The solvent used was HPLC-grade acetonitrile and degassed with nitrogen prior to each scan. All CV experiments were conducted using a 200 mV s^{-1} scan rate, in an electrolyte solution (tetrabutylammonium hexafluorophosphate, 0.1 M) with the compound of interest at 1 mM.

Stern-Volmer kinetic analysis was performed based on procedures previously described.[S3] The following equation and the results shown in Figure 3 and Figure S18 were used to calculate the quenching constant and the corresponding bimolecular rate constant.

$$\frac{I_0}{I} = 1 + K_{SV}[Q] = k_q \tau_0 [Q] \qquad \text{Eq. S2}$$

where I_0 and I were the fluorescence intensity without and with amine respectively, K_{SV} was the Stern-Volmer quenching constant, $[Q]$ was the concentration of the quencher in solution, k_q was the bimolecular rate constant, and τ_0 was the fluorescence lifetime without amine present.

Photographs were all taken with a Nikon D60 digital camera with a Tamron AF 18-200mm F/3.5-6.3 XR Di II LD Aspherical (IF) Macro lens. The black-light images were taken in a pitch-black room with a UVGL-25 Compact UV Lamp (P/N 95-0021-12, 4 watt, 365 nm) and an exposure time of between 6 and 10 seconds.

S2. Syntheses and Compound Characterizations

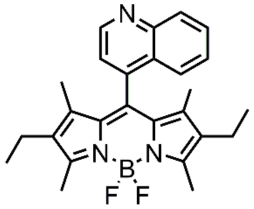

BQu: 3-Ethyl-2,4-dimethylpyrrole, **1**, (500 mg, 547 μL, 4.06 mmol) and 4-quinoline carboxaldehyde, **2**, (319 mg, 265 μL, 2.03 mmol) were dissolved in degased dichloromethane (200 mL) under argon. Three drops of trifluoroacetic acid (TFA) were added, and the solution was stirred at room temperature for 3 hours covered in tin foil. 2,3-Dichloro-5,6-dicyanoquinone (DDQ, 460 mg, 2.03 mmol) was added to the flask and the solution was stirred for 30 minutes, followed by the addition of BF_3•OEt_2 (6 mL) and trimethylamine (12 mL). This solution was stirred for 18 hours, washed with water (3 × 20 mL), dried over magnesium sulfate, and concentrated under vacuum. The crude product was purified by flash column chromatography with 5:1 hexane:ethyl acetate as eluent, and then HPLC (50 to 90%, acetonitrile to water (MeCN/H_2O) over 5 minutes, with a retention time of 8.7 minutes, buffered by 0.1% TFA). The pure fractions were concentrated, redissolved in dichloromethane, and washed with a 0.2 M sodium hydroxide solution to remove the TFA buffer. The washed organic layer was then dried with magnesium sulfate, and concentrated to yield the pure product, **BQu**, as a pink/red fluorescent solid (195.7 mg, 0.45 mmol, 22%). ^{1}H NMR (400 MHz, dichloromethane-d_2) δ = 9.01 (d, J = 4.3 Hz, 1H), 8.16 (d, J = 8.5 Hz, 1H), 7.85 – 7.73 (m, 2H), 7.52 (ddd, J = 8.3, 6.9, 1.3 Hz, 1H), 7.41 (d, J = 4.3 Hz, 1H), 2.52 (s, 6H), 2.34 – 2.19 (m, 4H), 1.03 (s, 6H), 0.94 (t, J =

7.5 Hz, 6H). ^{13}C NMR (126 MHz, dichloromethane-d$_2$) δ = 154.64, 150.34, 142.15, 137.98, 133.40, 130.27, 130.13, 129.83, 127.76, 127.04, 124.92, 121.30, 53.70, 16.91, 14.28, 12.39, 12.37, 11.10. ^{19}F NMR (376 MHz, dichloromethane-d$_2$) δ = –145.54 - –145.80 (m, 2F). HR-ESI-MS: $C_{26}H_{28}BF_2N_3$•H$^+$, Calculated: 432.2417, Found: 432.2416.

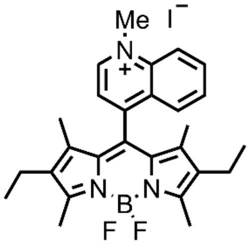

BQuMe•I: **BQu** (50 mg, 0.13 mmol) and iodomethane (10 μL, 0.16 mmol) were added to dry acetonitrile (MeCN, 5 mL) and stirred at room temperature for 2 days (until **BQu** was completely consumed, as confirmed by TLC) under tin foil. Prep-TLC was used for purification with ethyl acetate as eluent (maximum loading of 150 mg of material). **BQuMe**•I was recovered from the silica gel by washing with acetone (400 mL), and condensing to yield a dark red solid (65 mg, 0.11 mmol, 98%). ^{1}H NMR (400 MHz, dichloromethane-d$_2$) δ = 10.51 (d, *J* = 10.5 Hz, 1H), 8.41 (d, *J* = 8.8 Hz, 1H), 8.28 (dd, *J* = 9.8 & 7.7 Hz, 2H), 8.08 (d, *J* = 5.9 Hz, 1H), 7.96 (dd, *J* = 8.4 & 7.1 Hz, 1H), 4.96 (s, 3H), 2.55 (s, 5H), 2.28 (td, *J* = 7.5 & 1.5 Hz, 4H), 1.56 (s, 2H), 1.06 (s, 5H), 0.94 (t, *J* = 7.5 Hz, 5H). ^{13}C NMR (126 MHz, acetonitrile-d$_3$) δ = 156.32, 153.27, 149.96, 137.93, 136.60, 134.42, 131.87, 129.63, 129.04, 127.25, 123.05, 119.70, 46.41, 16.49, 13.78, 12.11, 11.40. ^{19}F NMR (376 MHz, dichloromethane-d$_2$) δ = –145.02 - –146.09 (m, 2F). HR-ESI-MS: $[C_{27}H_{31}BF_2N_3^+ \bullet I^-] \bullet I^-$, Calculated: 700.0674, Found: 700.0650.

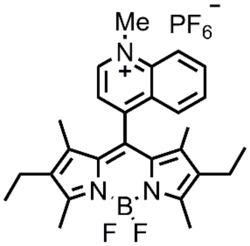

BQuMe•PF$_6$: **BQuMe**•I (50 mg, 0.13 mmol) was dissolved in acetonitrile (5 mL) and added dropwise to 250 mL of 0.2 M potassium hexafluorophosphate. This solution was stirred for 10 minutes, during which the product precipitated out of solution. The product was filtered, washed with water and dried under vacuum, providing **BQuMe**•PF$_6$ as a dark red solid (52 mg, 0.09 mmol, quantitative). ^{1}H NMR (400 MHz, dichloromethane-d$_2$) δ = 9.36 (d, *J* = 6.0 Hz, 1H), 8.42 – 8.28 (m, 3H), 8.07 (d, *J* = 5.9 Hz, 1H), 8.00 (t, *J* = 7.8 Hz, 1H), 4.83 (s, 3H), 2.34 – 2.23 (m, 4H), 1.26 (s, 6H), 1.00 (s, 6H), 0.95 (t, *J* = 7.6 Hz, 6H). ^{13}C NMR (126 MHz, dichloromethane-d$_2$) δ = 156.95, 149.47, 137.32, 137.18, 134.73, 131.96, 129.55, 128.22, 123.00, 118.74, 53.68, 53.02, 46.71, 16.93, 14.16, 12.60, 11.84. ^{19}F NMR (376 MHz, dichloromethane-d$_2$) δ = –72.87 (d, *J* = 710.7 Hz, 6F), –145.06 - –146.05 (m, 2F). HR-ESI-MS: $[C_{27}H_{31}BF_2N_3^+ \bullet PF_6^-] \bullet PF_6^-$, Calculated: 736.1868, Found: 736.1868.

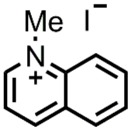

QuMe•I: Quinoline (1 g, 914 μL, 7.7 mmol) was added to acetonitrile (5 mL) along with iodomethane (2.1 g, 960 μL, 15.5 mmol) and the mixture was left to stir overnight. Solid product (yellow powder) crashed out of solution and was collected by filtration. The product was further purified by recrystallization from hot methanol (2 g, 7.7 mg, 95% yield). ^{1}H NMR (400 MHz, acetonitrile-d$_3$) δ = 9.17 (d, *J* = 5.8 Hz, 1H), 9.12 (d, *J* = 8.4 Hz, 1H), 8.42 – 8.35 (m, 2H), 8.27 (ddd, *J* = 8.8, 7.0, 1.4 Hz, 1H), 8.08 – 7.99 (m, 2H), 4.59 (s, 3H). ^{13}C NMR (126 MHz, acetonitrile-d$_3$) δ = 149.69, 147.66, 138.98, 135.95, 130.57, 130.33, 129.80, 121.82, 118.70, 45.69. HR-ESI-MS: [$C_{10}H_{10}N^+$], Calculated: 144.0813, Found: 144.0808.

S3. X-Ray Crystallography of BQuMe•PF$_6$

The data collection was carried out using Mo K$_\alpha$ radiation (graphite monochromator) with a frame time of 60 seconds and a detector distance of 4.00 cm. A collection strategy was calculated and complete data to a resolution of 0.80 Å with a redundancy of 4 were collected. Five major sections of frames were collected with 0.50º ω and ϕ scans; details are given below.

Axis	**2θ/°**	**ω/°**	**φ/°**	**χ/°**	**Frames**
Phi	–15.50	–15.59	–12.14	–28.13	739
Phi	9.50	41.14	–10.45	–24.37	219
Omega	–25.50	–30.30	77.78	–71.54	75
Omega	–23.00	–27.59	–265.55	–98.73	94
Omega	19.50	–39.84	–93.66	96.91	126

A total of 1253 frames were collected. The total exposure time was 20.88 hours. The frames were integrated with the Bruker SAINT software package[S4] using a narrow-frame algorithm. The integration of the data using a triclinic unit cell yielded a total of 14058 reflections to a maximum θ angle of 25.12° (0.84 Å resolution), of which 5356 were independent (average redundancy 2.625, completeness = 99.3%, R_{int} = 6.95%, R_{sig} = 11.94%) and 2669 (49.83%) were greater than 2σ(F_2). The final cell constants of *a* = 7.9585(5) Å, *b* = 9.4240(5) Å, *c* = 20.5726(13) Å, *α* = 86.645(3)°, *β* = 79.638(3)°, *γ* = 84.679(3)°, volume = 1509.88(16) Å^3, are based upon the refinement of the XYZ-centroids of 2104 reflections above 20 σ(*I*) with 4.344° < 2θ < 44.20°. Data were corrected for absorption effects using the multi-scan method (SADABS).[S5] The ratio of minimum to maximum apparent transmission was 0.833. The calculated minimum and maximum transmission coefficients (based on crystal size) are 0.6210 and 0.7452. Please refer to Table S1 for additional crystal and refinement information.

The space group *P*-1 was determined based on intensity statistics and the lack of systematic absences. The structure was solved and refined using the SHELX suite of programs.[S6] An intrinsic-methods solution was calculated, which provided most non-hydrogen atoms from the E-map. Full-matrix least squares / difference Fourier cycles were performed, which located the remaining non-hydrogen atoms. All non-hydrogen atoms were refined with anisotropic displacement parameters. The hydrogen atoms were placed in ideal positions and refined as riding atoms with relative isotropic displacement parameters. Disorder was refined for the co-crystalized solvent molecule (DCM). The final anisotropic full-matrix least-squares refinement on F_2 with 405 variables converged at R_1 = 7.99%, for the observed data and wR_2 = 27.36% for all data. The goodness-of-fit was 1.007. The largest peak in the final difference electron density synthesis was 0.626 $e^{-}/Å^3$ and the largest hole was –0.991 $e^{-}/Å^3$ with an RMS deviation of 0.097 $e^{-}/Å^3$. On the basis of the final model, the calculated density was 1.487 g/cm^3 and $F(000)$, 696 e^{-}. The remaining electron density is minuscule and located on bonds.

Table S1. Crystal data and structure refinement for **BQuMe•**PF_6.

Empirical formula	$C_{28}\,H_{33}\,B\,Cl_{2}\,F_{8}\,N_{3}\,P$	
Formula weight	676.25	
Crystal color, shape, size	red plate, 0.23 × 0.11 × 0.03 mm^3	
Temperature	173(2) K	
Wavelength	0.71073 Å	
Crystal system, space group	Triclinic, P-1	
Unit cell dimensions	a = 7.9585(5) Å	α = 86.645(3)°
	b = 9.4240(5) Å	β = 79.638(3)°
	c = 20.5726(13) Å	γ = 84.679(3)°
Volume	1509.88(16) $Å^3$	
Z	2	
Density (calculated)	1.487 mg/m^3	
Absorption coefficient	0.343 mm^{-1}	
$F(000)$	696	

Data collection

Diffractometer	APEX II Kappa Duo, Bruker
Theta range for data collection	1.007 to 25.119°.
Index ranges	$-9 \leq h \leq 9, -11 \leq k \leq 8, -24 \leq l \leq 24$
Reflections collected	14058
Independent reflections	5356 [R_{int} = 0.0695]
Observed Reflections	2669
Completeness to theta = 25.119°	99.3 %

Solution and Refinement

Absorption correction	Semi-empirical from equivalents
Max. and min. transmission	0.7452 and 0.6210
Solution	Intrinsic methods
Refinement method	Full-matrix least-squares on F^2
Weighting scheme	$w = [\sigma^2 F_o^2 + AP^2]^{-1}$, with $P = (F_o^2 + 2\,F_c^2) / 3$, $A = 0.1537$
Data / restraints / parameters	5356 / 7 / 405
Goodness-of-fit on F^2	1.007
Final R indices [I > 2sigma(I)]	R_1 = 0.0799, wR_2 = 0.2179
R indices (all data)	R_1 = 0.1668, wR_2 = 0.2736
Largest diff. peak and hole	0.626 and –0.991 e.$Å^{-3}$

Goodness-of-fit = $[\Sigma[w(F_o^2 - F_c^2)^2] / N_{observns} - N_{params})]^{1/2}$, all data.

$R_1 = \Sigma(|F_o| - |F_c|) / \Sigma\,|F_o|$. $wR_2 = [\Sigma[w(F_o^2 - F_c^2)^2] / \Sigma\,[w(F_o^2)^2]]^{1/2}$.

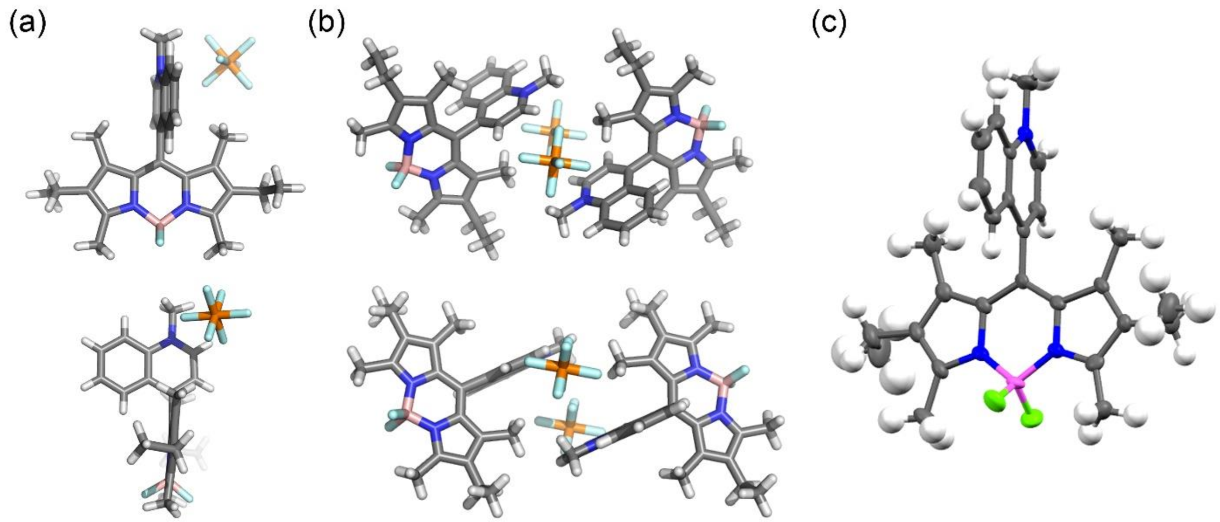

Figure S1. (a) The crystal structure of **BQuMe**•PF_6, highlighting two profiles of the structure. Disorder and solvent molecules are omitted. (b) The packing in one unit cell within the **BQuMe**•PF_6 crystal structure, highlighting three profiles of the unit cell. (c) Ellipsoid figure of **BQuMe**$^+$ to show atom placement. Disorder and solvent molecules are omitted.

S4. Characterization of the Sensing Properties

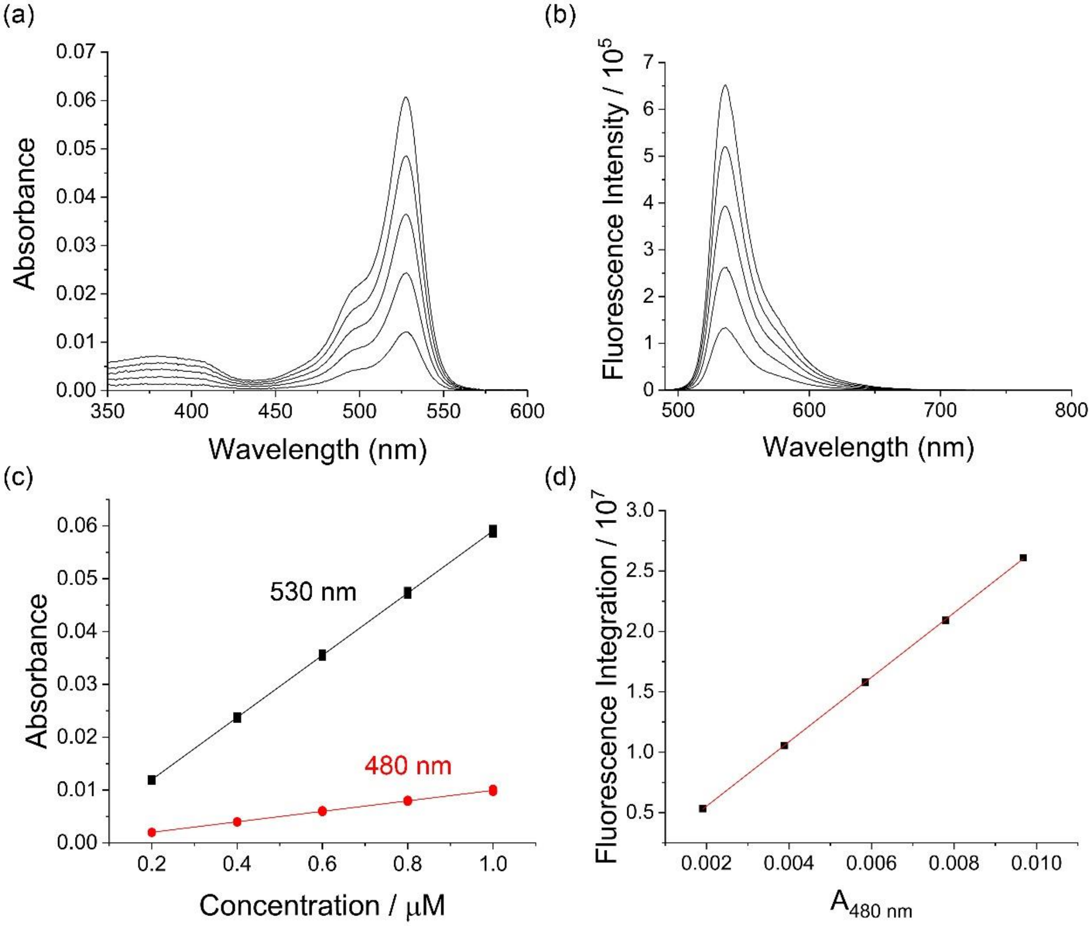

Figure S2. (a) The stacked absorbance spectra of variable concentration **BQu** in MeCN; (b) stacked fluorescence emission spectra of variable concentration **BQu** in MeCN with an excitation of 480 nm; (c) Beer's Law plot of absorbance at 480 nm (ε_{480} = 1000 M^{-1} cm^{-1}; R^2 = 0.9969) and 530 nm (ε_{530} = 60000 M^{-1} cm^{-1}; R^2 = 0.9997); (d) fluorescence emission peak integration versus the absorbance at 480 nm of **BQu** in MeCN for quantum yield determination. The concentrations used were 0.2, 0.4, 0.6, 0.8, and 1.0 μM. The standard used was rhodamine 6G in methanol, with a quantum yield of 0.94.[S1]

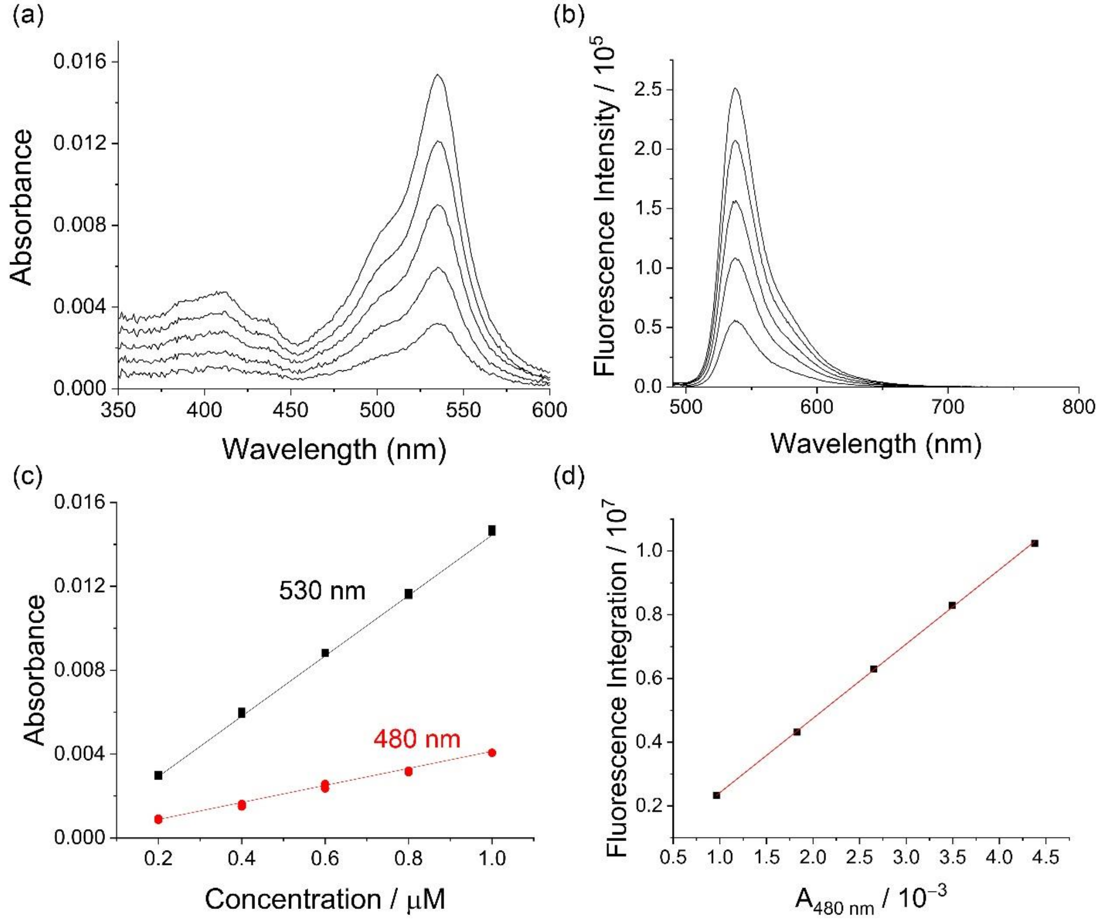

Figure S3. (a) The stacked absorbance spectra of variable concentration **BQuMe•**PF_6 in MeCN; (b) stacked fluorescence emission spectra of variable concentration **BQuMe•**PF_6 in MeCN with an excitation of 480 nm; (c) Beer's Law plot of absorbance at 480 nm (ε_{480} = 4000 M^{-1} cm^{-1}; R^2 = 0.9869) and 530 nm (ε_{530} = 14000 M^{-1} cm^{-1}; R^2 = 0.9972); (d) fluorescence emission peak integration versus the absorbance at 480 nm of **BQuMe•**PF_6 in MeCN for quantum yield determination. The concentrations used were 0.2, 0.4, 0.6, 0.8, and 1.0 μM. The standard used was ruthenium(II) trisbypyridine dichloride in acetonitrile, with a quantum yield of 0.018.[S2]

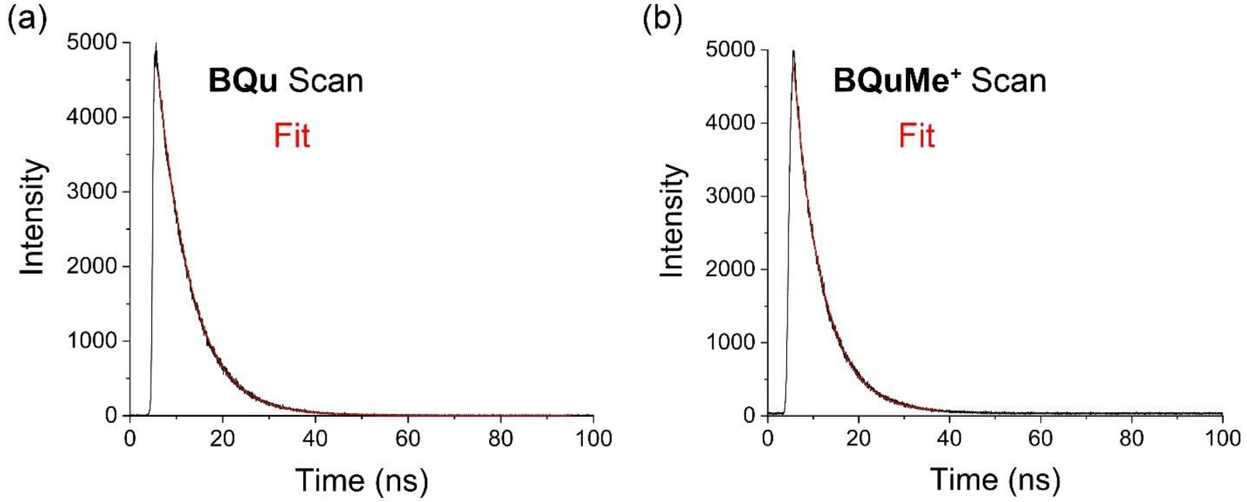

Figure S4. Fluorescence lifetime decay spectra of (a) **BQu** (1 μM) and (b) **BQuMe**$^+$ (1 μM) in MeCN with corresponding fits.

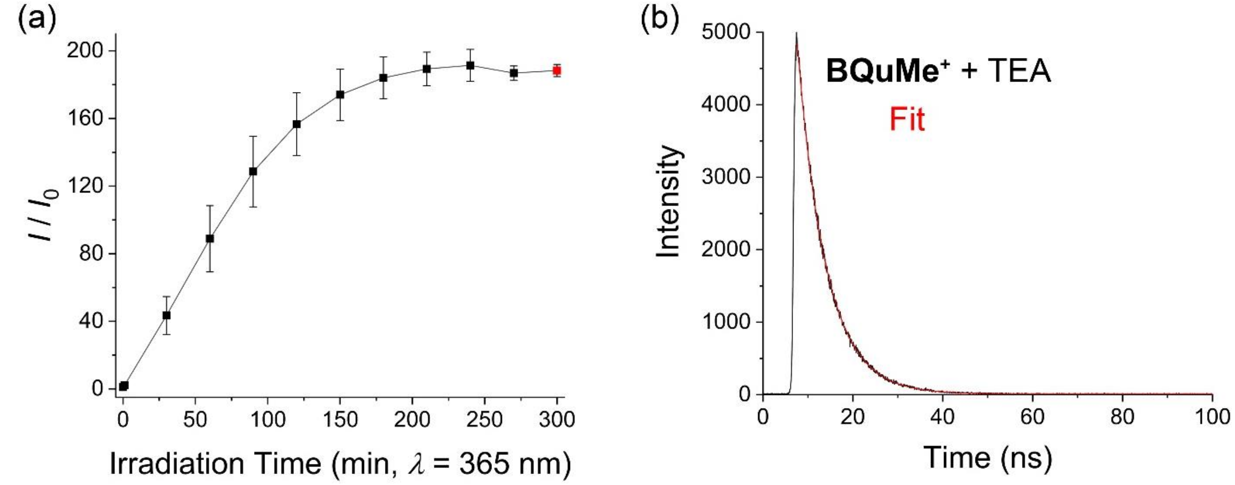

Figure S5. (a) Plot of the ratio of the fluorescence emission intensity of **BQuMe**$^+$ (1 μM) as a function of time with 5 mM TEA in MeCN, degassed with argon and irradiated with UV light (λ = 365 nm) between time points. (b) Fluorescence lifetime decay spectrum and fit of **BQuMe**$^+$ (1 μM, MeCN) with 5 mM TEA, degassed with argon and irradiated with UV light (λ = 365 nm) for 300 minutes.

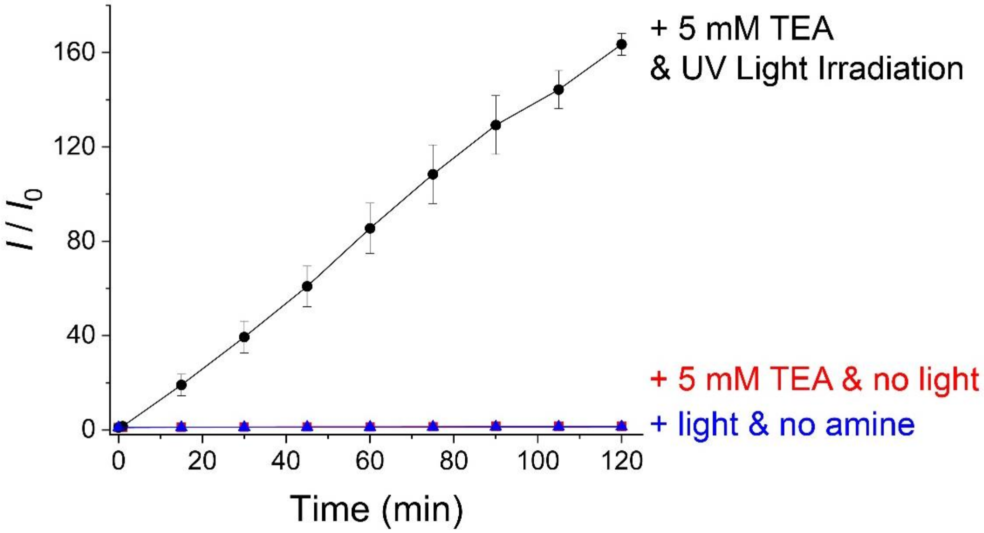

Figure S6. Plot of the ratio of the fluorescence emission intensity of **BQuMe**$^+$ (1 μM, MeCN) as a function of time, degassed with argon. With 5 mM TEA in MeCN and irradiated with UV light (λ = 365 nm, black) between time points, without light (red) and without amine (blue).

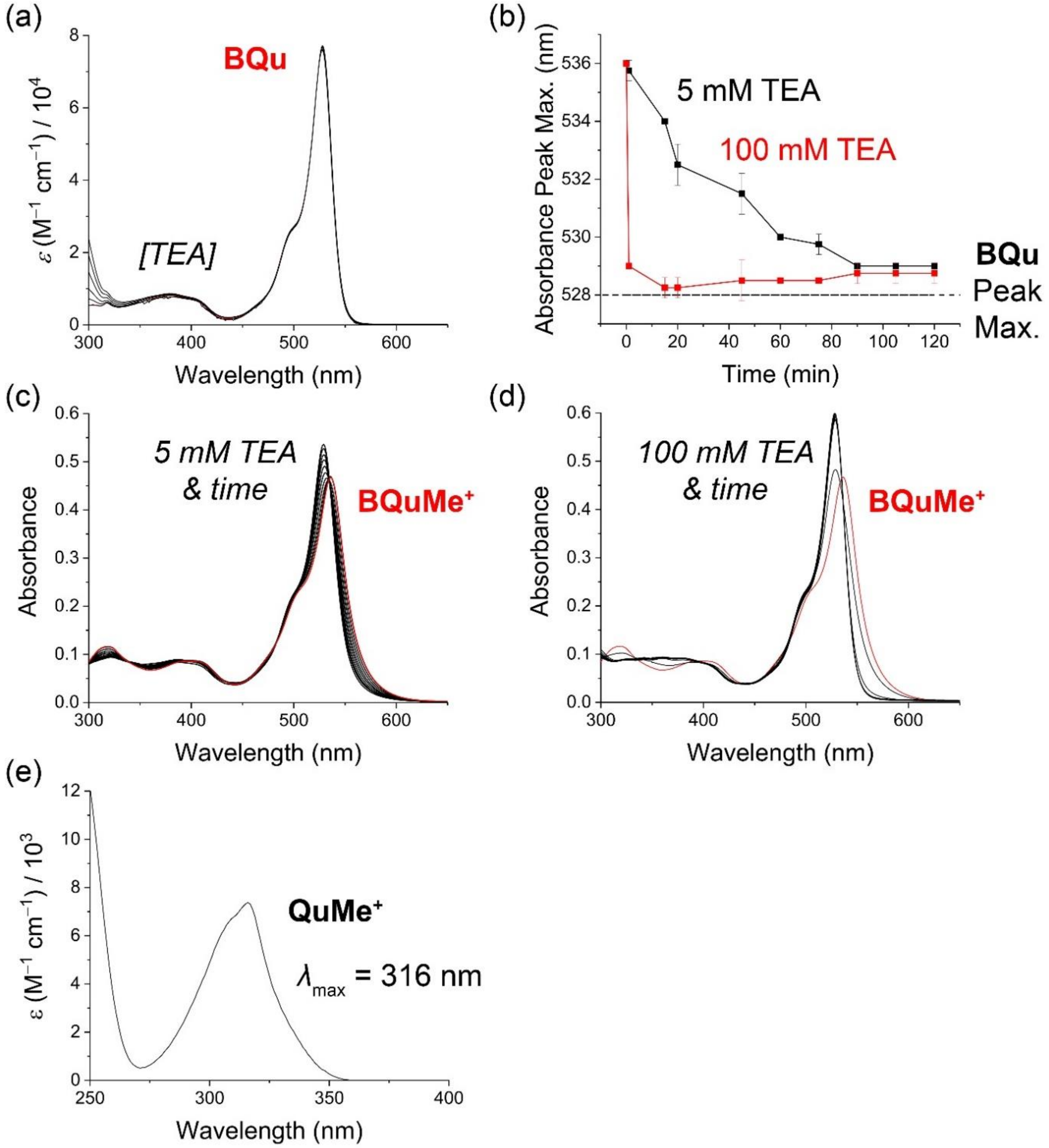

Figure S7. UV-Vis analysis of **BQuMe**$^+$ and **BQu** in response to triethylamine. (a) Concentration corrected absorbance spectra of **BQu** (10 μM, MeCN, degassed with argon) without and with triethylamine (5 mM, 100 mM, 250 mM, 500 mM, 750 mM, and 1 M). (b) A comparison of the shift in absorption peak maxima position for **BQuMe**$^+$ over time with 5 mM (black trace) and 100 mM (red trace) of triethylamine; duplicated. (c) Representative absorption spectra of **BQuMe**$^+$ (red trace, 10 μM, MeCN, degassed with argon) changing over 120 minutes in the presence of triethylamine (5 mM), irradiated with UV light (λ = 365 nm) between scans. (d) Representative absorption spectra of **BQuMe**$^+$ (red trace, 10 μM, MeCN, degassed with argon) changing over 120 minutes in the presence of triethylamine (100 mM), irradiated with UV light (λ = 365 nm) between scans. (e) Average molar absorptivity of **QuMe**$^+$ (MeCN, from duplicated spectra collected at 5, 10, and 20 μM).

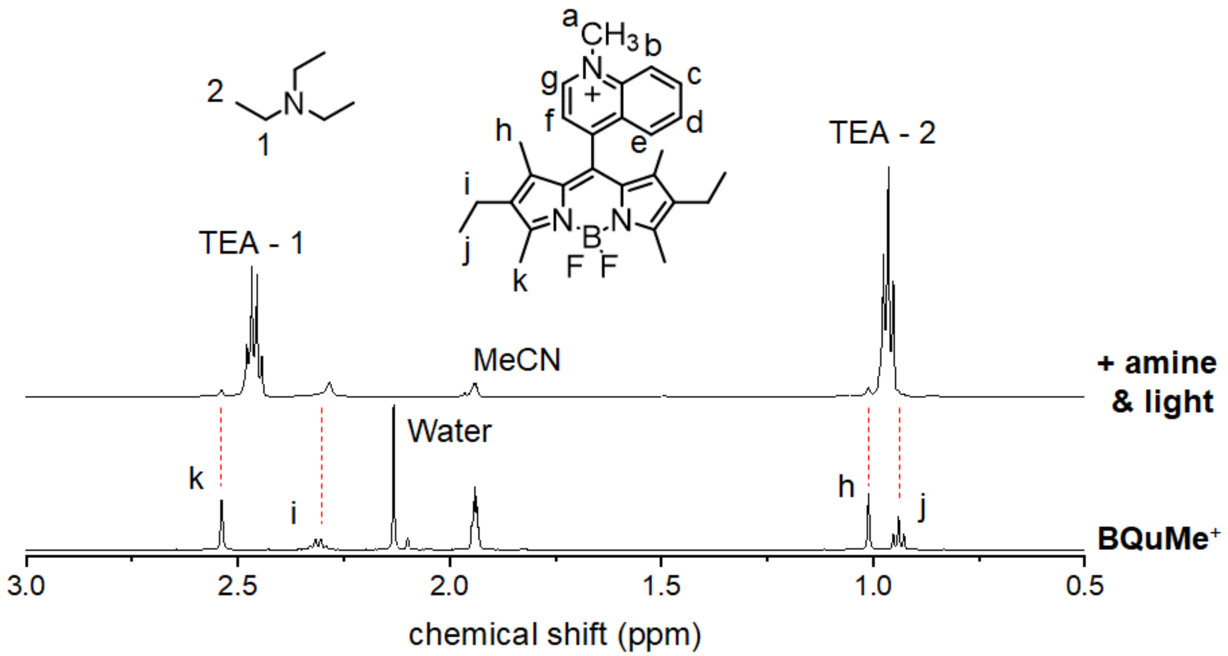

Figure S8. Zoomed ^{1}H NMR of **BQuMe**$^+$ (5 mM, MeCN-*d*) before and after adding triethylamine (100 mM) and UV irradiation (λ = 365 nm, 90 minutes).

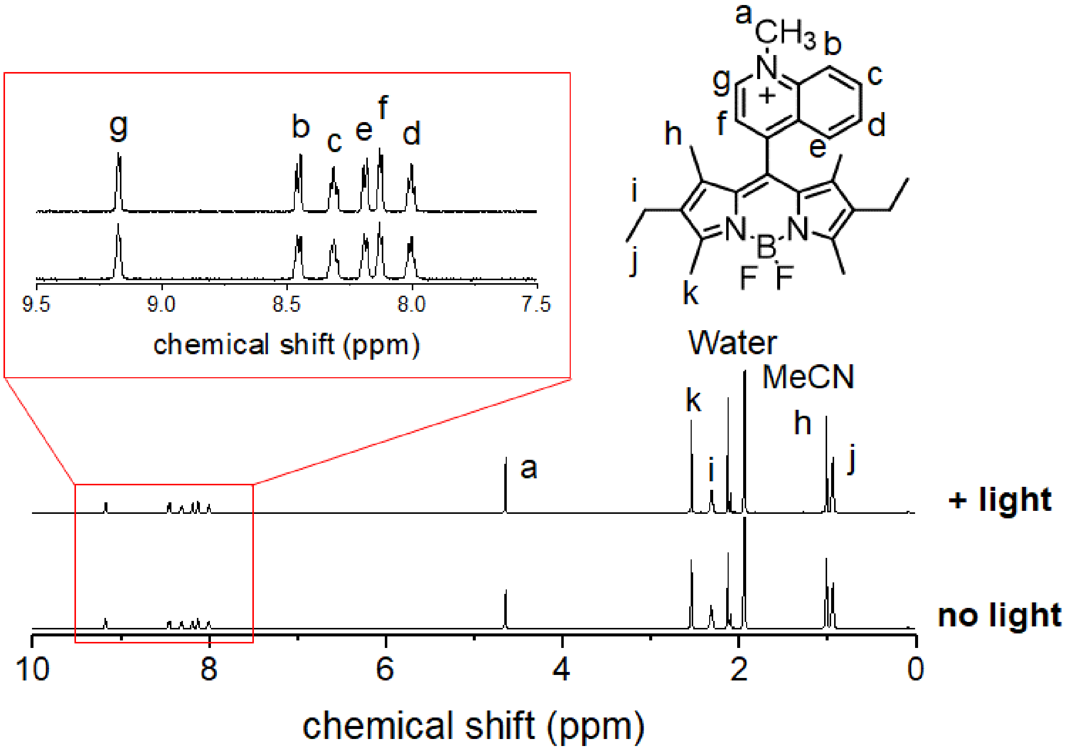

Figure S9. ^{1}H NMR of **BQuMe**$^+$ (5 mM, MeCN-*d*) before and after UV irradiation (λ = 365 nm, 120 minutes) showing no change in signal.

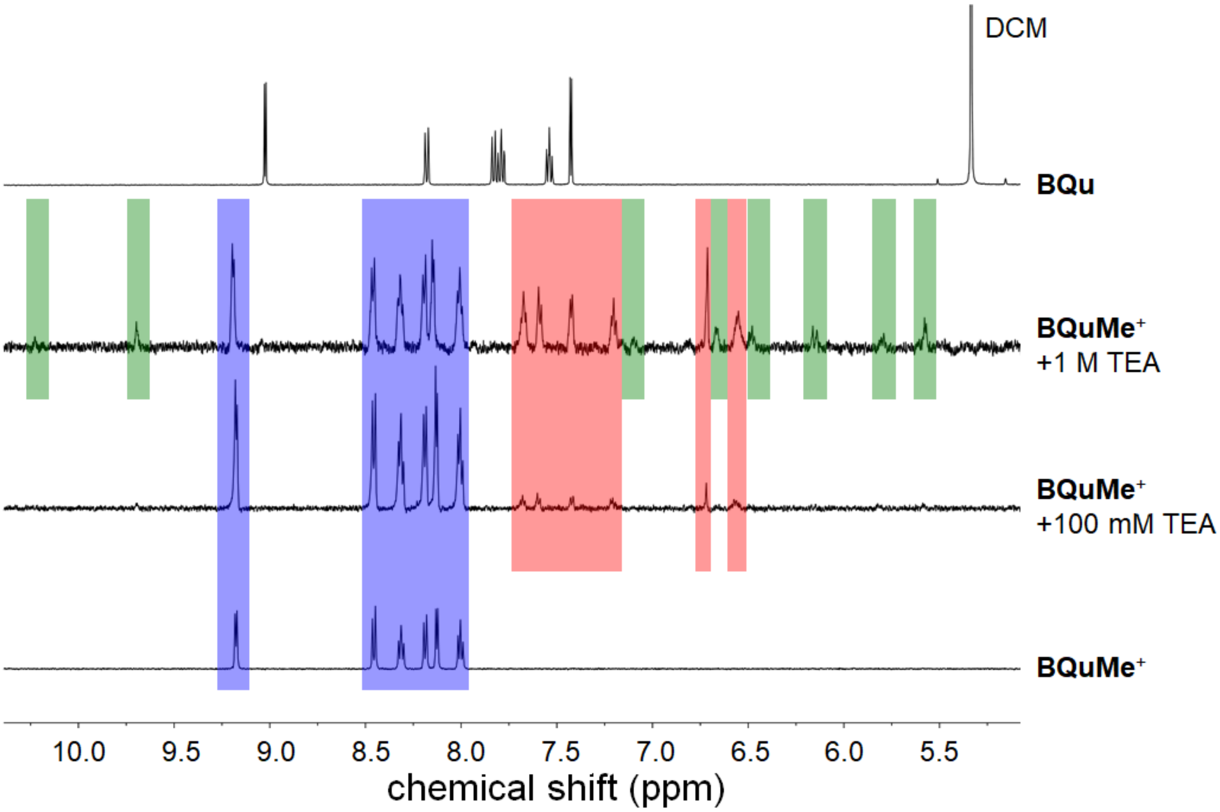

Figure S10. ^{1}H NMR of **BQu** (5 mM, DCM-*d*) in comparison with **BQuMe**$^+$ (5 mM, MeCN-*d*, degassed with argon) before and after addition of 100 mM and 1 M triethylamine (90 minutes, UV irradiation, λ = 365 nm). Highlighting placed on the **BQuMe**$^+$ quinolinium peaks (blue), first decomposition product peaks (red), and second decomposition product peaks (green), none of which align with the peaks for **BQu**.

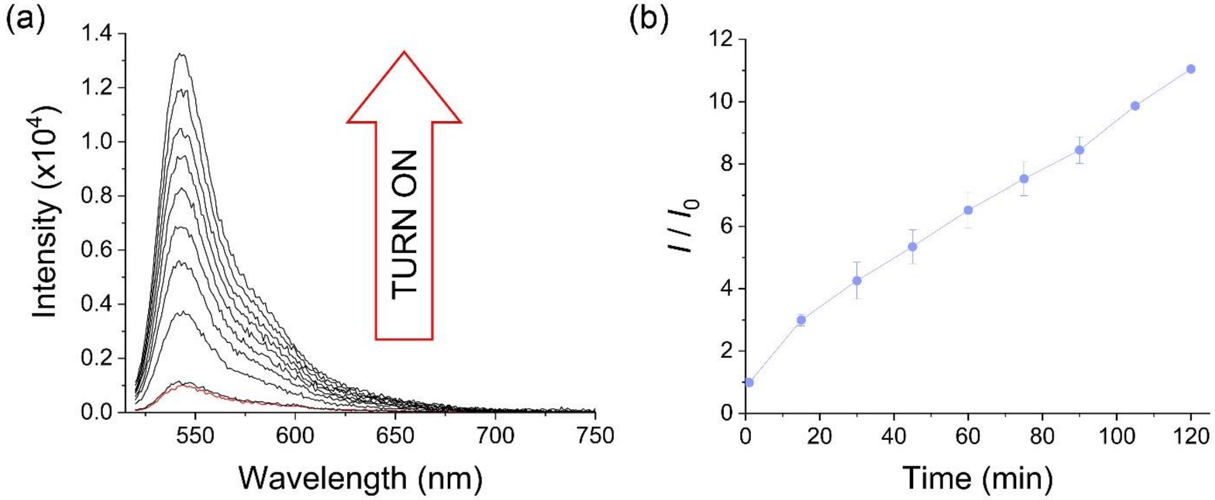

Figure S11. (a) Representative stacked fluorescence emission spectra of **BQuMe**$^+$ (1 μM, degassed with argon, MeCN, λ_{exc} = 510 nm, red line) with triethylamine (0.1 mM) and UV irradiation (λ = 365 nm) increasing over time (black lines). (b) The corresponding change in fluorescence peak maximum intensity of **BQuMe**$^+$ (1 μM, degassed with argon, MeCN, λ_{exc} = 510 nm) over time with 0.1 mM triethylamine and UV irradiation (λ = 365 nm); error bars included based off of the standard deviation from at least two replicate experiments.

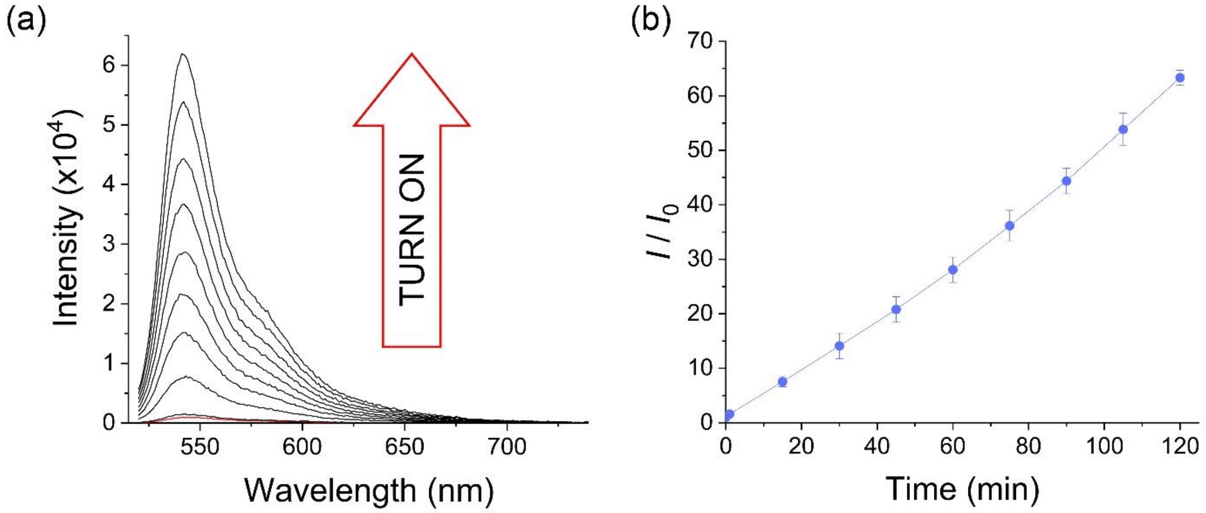

Figure S12. (a) Representative stacked fluorescence emission spectra of **BQuMe**$^+$ (1 μM, degassed with argon, MeCN, λ_{exc} = 510 nm, red line) with triethylamine (1 mM) and UV irradiation (λ = 365 nm) increasing over time (black lines). (b) The corresponding change in fluorescence peak maximum intensity of **BQuMe**$^+$ (1 μM, degassed with argon, MeCN, λ_{exc} = 510 nm) over time with 1 mM triethylamine and UV irradiation (λ = 365 nm); error bars included based off of the standard deviation from at least two replicate experiments.

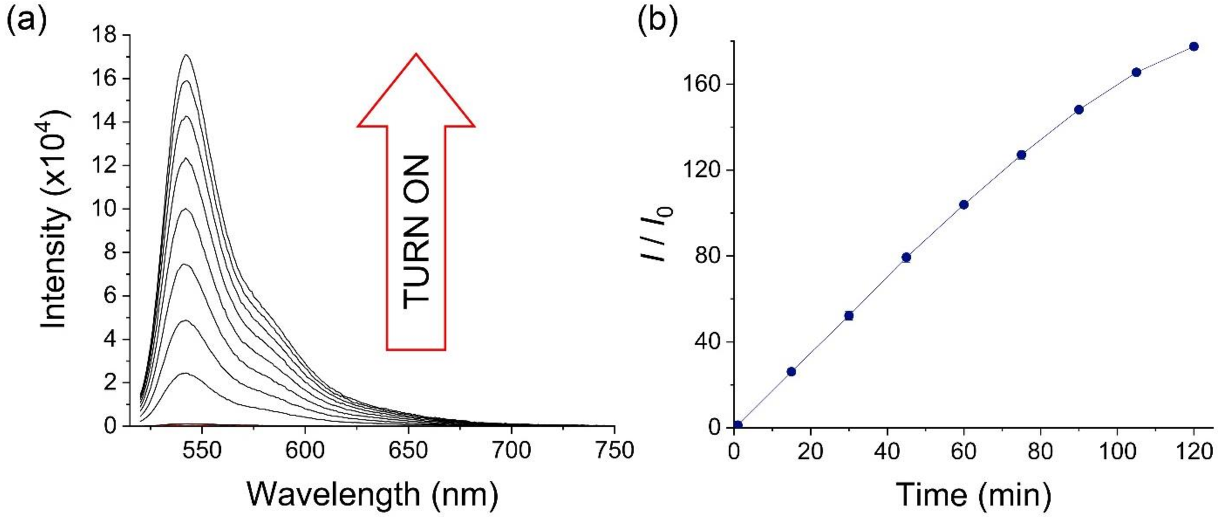

Figure S13. (a) Representative stacked fluorescence emission spectra of **BQuMe**$^+$ (1 μM, degassed with argon, MeCN, λ_{exc} = 510 nm, red line) with triethylamine (10 mM) and UV irradiation (λ = 365 nm) increasing over time (black lines). (b) The corresponding change in fluorescence peak maximum intensity of **BQuMe**$^+$ (1 μM, degassed with argon, MeCN, λ_{exc} = 510 nm) over time with 10 mM triethylamine and UV irradiation (λ = 365 nm); error bars included based off of the standard deviation from at least two replicate experiments.

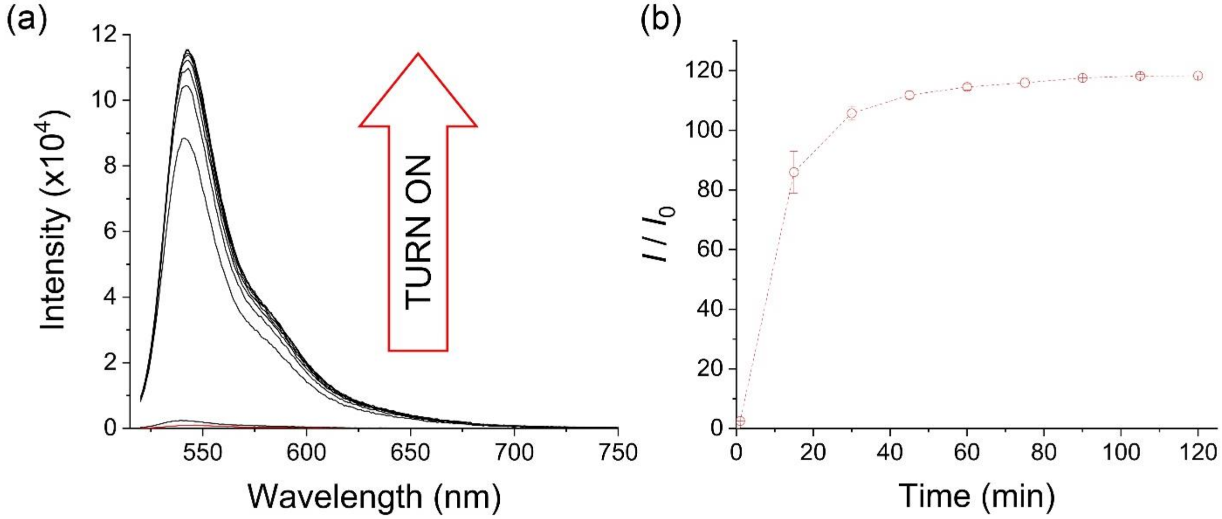

Figure S14. (a) Representative stacked fluorescence emission spectra of **BQuMe**$^+$ (1 μM, degassed with argon, MeCN, λ_{exc} = 510 nm, red line) with triethylamine (50 mM) and UV irradiation (λ = 365 nm) increasing over time (black lines). (b) The corresponding change in fluorescence peak maximum intensity of **BQuMe**$^+$ (1 μM, degassed with argon, MeCN, λ_{exc} = 510 nm) over time with 50 mM triethylamine and UV irradiation (λ = 365 nm); error bars included based off of the standard deviation from at least two replicate experiments.

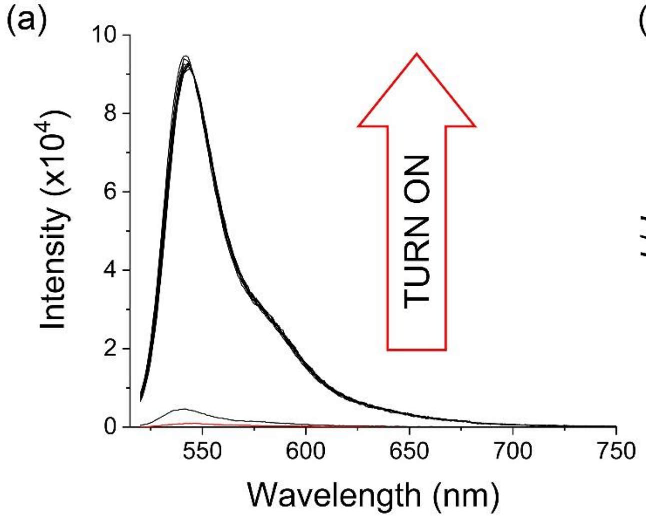

Figure S15. (a) Representative stacked fluorescence emission spectra of **BQuMe**$^+$ (1 μM, degassed with argon, MeCN, λ_{exc} = 510 nm, red line) with triethylamine (100 mM) and UV irradiation (λ = 365 nm) increasing over time (black lines). (b) The corresponding change in fluorescence peak maximum intensity of **BQuMe**$^+$ (1 μM, degassed with argon, MeCN, λ_{exc} = 510 nm) over time with 100 mM triethylamine and UV irradiation (λ = 365 nm); error bars included based off of the standard deviation from at least two replicate experiments.

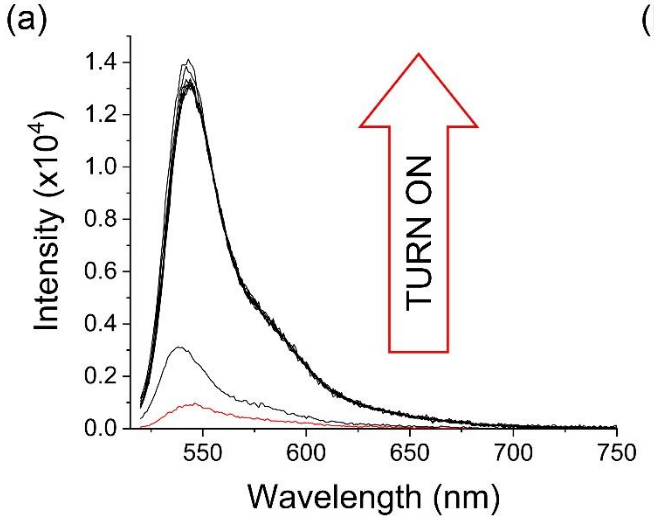

Figure S16. (a) Representative stacked fluorescence emission spectra of **BQuMe**$^+$ (1 μM, degassed with argon, MeCN, λ_{exc} = 510 nm, red line) with triethylamine (1 M) and UV irradiation (λ = 365 nm) increasing over time (black lines). (b) The corresponding change in fluorescence peak maximum intensity of **BQuMe**$^+$ (1 μM, degassed with argon, MeCN, λ_{exc} = 510 nm) over time with 1 M triethylamine and UV irradiation (λ = 365 nm); error bars included based off of the standard deviation from at least two replicate experiments.

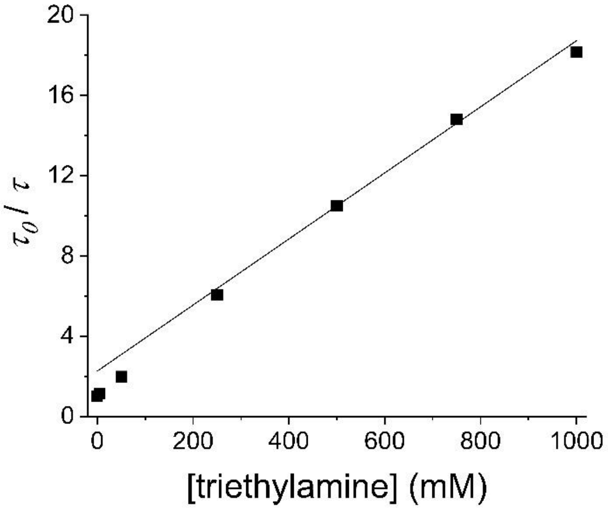

Figure S17. Stern-Volmer plot of the change in fluorescence lifetime of **BQu** (1 µM, MeCN) upon addition of triethylamine with linear fit ($R^2 = 0.99$).

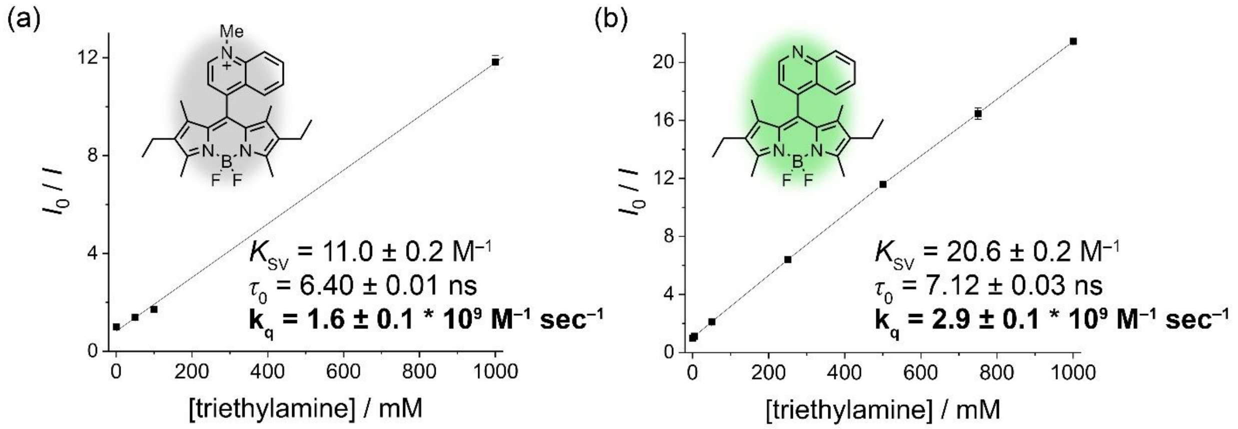

Figure S18. Stern-Volmer plot of the change in fluorescence intensity for (a) **BQuMe$^+$** (1 µM, MeCN) and (b) **BQu** (1 µM, MeCN) at high amine concentrations (> 50 mM) with corresponding linear fits, Stern-Volmer constant, fluorescence lifetime, and collisional quenching constant. The plot for **BQuMe$^+$** was generated by assuming that the I_0 intensity was intensity at the maximum turn-on response generated by 5 mM of amine after five hours (see Figure 3).

S5. Time-Dependent Density Functional Theory (TDDFT)

All computations have been carried out Gaussian 16 program package.[S7] The probe, **BQuMe•**PF_6, was modeled as a free cation, **BQuMe**$^+$. Acetonitrile (ε = 35.7) solvation was implicitly considered for all calculations using the CPCM model.[S8] The ground state (S_0) geometry optimization was performed using B3LYP-D3BJ functional and a 6-31+G(d,p) basis set. Vibrational analyses were conducted with the same level of theory as the ground state to verify the stationary points to be minimum energy structures. Single-point energies and the frontier molecular orbitals (FMOs) were calculated at the CAM-B3LYP/6-311++G(3df,2p) level of theory.

Table S2. Summary of vertical excitations using ground-state geometries (CAM-B3LYP/6-311++g(3df,2p), CPCM:MeCN).

Fluorophore	Vertical Transitions	Associated Orbitals	Character[a]	Energy (eV)	f^b	Contribution[c]
BQu	$S_0 \rightarrow S_1$	HOMO→LUMO	LE	2.49	0.89	0.98
	$S_0 \rightarrow S_2$	HOMO–2→LUMO	LE	3.61	0.09	0.96
	$S_0 \rightarrow S_3$	HOMO→LUMO+1	CT	3.85	0.01	0.96
BQuMe$^+$	$S_0 \rightarrow S_1$	HOMO→LUMO+1	LE	2.45	0.89	0.97
	$S_0 \rightarrow S_2$	HOMO→LUMO	CT	2.69	0.01	0.96

[a] LE: local excitation; CT: charge transfer.
[b] *f* = oscillator strength
[c] Contributions are from natural transition orbital (NTO) analysis.

The optimization of the excited state geometries and the calculations of vertical excitation energy were performed using time-dependent density functional theory (TDDFT). To evaluate the first excited state geometry (S_1), six low-lying singlet excited states were solved at each geometry point using a B3LYP-D3BJ/6-31+G(d,p) level of theory. No constraints on the symmetry, bonds, angles, or dihedral angles were applied in the S_0 and S_1 geometry optimizations. Vertical excitation and emission energies were analyzed at the CAM-B3LYP/6-311++G(3df,2p) level of theory for the S_0 and S_1 optimized geometries. Further, the Multiwfn program was used to generate natural transition orbitals (NTOs).

Table S3. Summary of vertical transitions corresponding to emissions using excited-state geometries (CAM-B3LYP/6-311++g(3df,2p), CPCM:MeCN).

Fluorophore	Vertical Transitions	Associated Orbitals	Character[a]	Energy (eV)	f^b	Contribution[c]
BQu	$S_1 \rightarrow S_0$	LUMO→HOMO	LE	2.33	0.78	0.97
	$S_2 \rightarrow S_0$	LUMO→HOMO–2	LE	3.47	0.08	0.96
	$S_3 \rightarrow S_0$	–	Mixed	3.70	0.39	0.92
	$S_4 \rightarrow S_0$	–	Mixed	3.76	0.01	0.92
	$S_5 \rightarrow S_0$	LUMO+1→HOMO	CT	3.86	0.05	0.89
BQuMe$^+$	$S_1 \rightarrow S_0$	LUMO→HOMO	CT	2.20	0.03	0.97
	$S_2 \rightarrow S_0$	LUMO+1→HOMO	LE	2.44	0.87	0.97

[a] LE: local emission; CT: charge transfer.

[b] f = oscillator strength

[c] Contributions are from natural transition orbital (NTO) analysis.

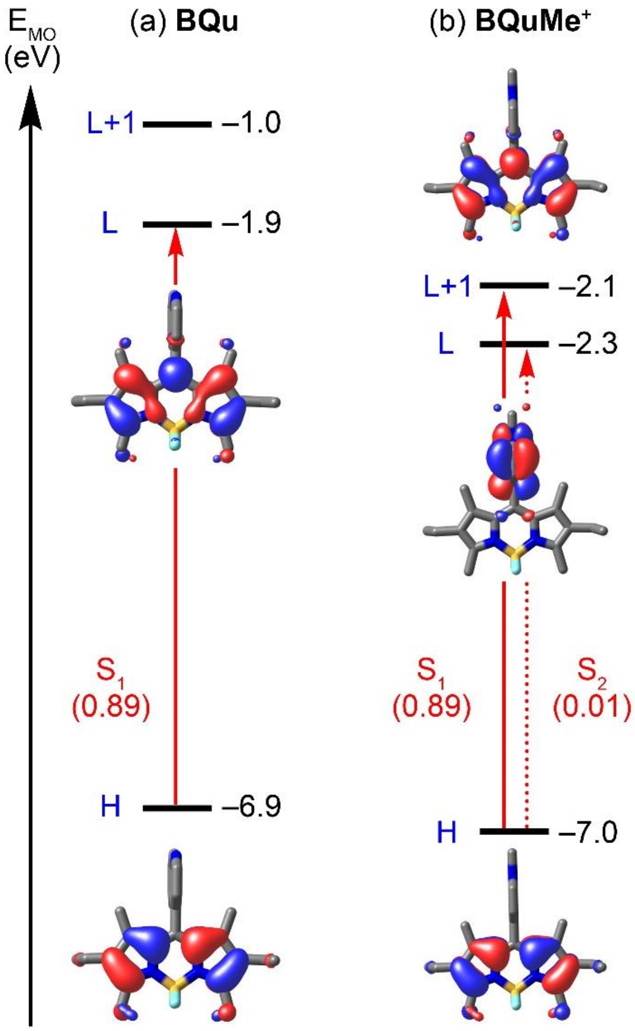

Figure S19. Vertical transitions calculated using TDDFT for the excitations of (a) **BQu** and (b) **BQuMe**$^+$ with solvation (acetonitrile). All vertical transitions were dominated by a single electronic transition (Tables S2 and S3). The orbitals shown are from natural transition orbital analysis. Oscillator strengths for the electronic transitions are included in parentheses; solid lines indicate higher oscillator strengths and dashed lines indicate lower oscillator strengths.

The reliability of CAM-B3LYP method to calculate the excited state geometries and energies was confirmed by the high consistency between computed UV-Vis absorption spectra and the experimental spectra (Figure S20). We noticed the molar absorptivity for **BQu** (60,000 M^{-1} cm^{-1}) and **BQuMe**$^+$ (14,000 M^{-1} cm^{-1}) were significantly different. To verify these values, we used ^{1}H NMR spectroscopy and the acetonitrile solvent as the internal standard to verify the solution concentrations of 5 mM. The acetonitrile has a concentration of 1.9 M (based on volume, density, and mass), which was corrected to account for the amount of non-deuterated solvent in the solution (1%). The integration for the solvent was compared to the integrations of every unique proton on the probe (Table S4). Note that long relaxation times were not used, so some error may be from differences in relaxation time between aromatic and aliphatic protons.

Overall, the average concentration determine for both **BQuMe**•PF_6 and **BQuMe**•I is consistent with the expected 5 mM (within 10% error).

Table S4. Integrations for the acetonitrile peaks and compound peaks, confirming the solution concentrations for the probes (within 10%).

		BQuMe•PF_6		**BQuMe**•I	
	Peak Label*	Peak Integration	Concentration (mM)	Peak Integration	Concentration (mM)
	Acetonitrile (3H)	12.0886	19147.38	8.8069	19147.38
Aromatic	A (1H)	1.0000	4.75	1.0000	6.52
	B (1H)	1.0426	4.95	1.0424	6.80
	C (1H)	1.0625	5.05	1.1450	7.47
	D (1H)	0.9752	4.63	0.9458	6.17
	E (1H)	1.0056	4.78	0.8862	5.78
	F (1H)	1.0616	5.04	1.1382	7.42
Aliphatic	G (3H)	2.9310	4.64	2.3526	5.11
	H (6H)	5.6064	4.44	4.5566	4.95
	I (4H)	4.1306	4.91	3.4390	5.61
	J (6H)	5.2188	4.13	4.3500	4.73
	K (6H)	5.9651	4.72	4.9622	5.39
Avg. Concentration (mM) →			4.73		5.16

*the peaks for the ^1H signals on **BQuMe**$^+$ are labeled on the structure below:

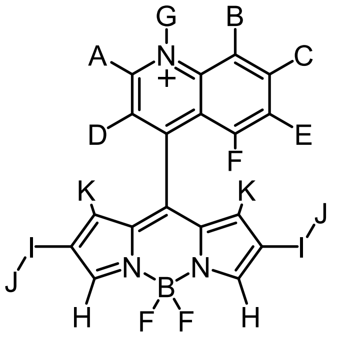

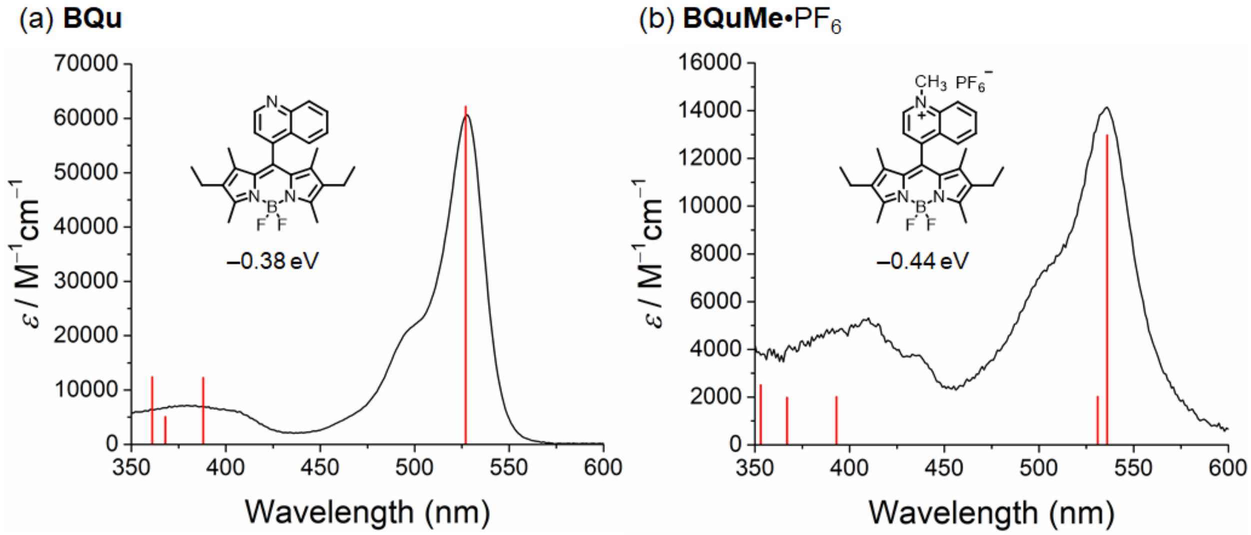

Figure S20. Comparison between computed and experimental absorption spectra. Extinction spectra were used as the experimental spectra (black spectra). The computed spectra are represented by bars (red lines), which correspond to the relative oscillator strength of the electronic transitions.

S6. ^{1}H, ^{13}C, and ^{19}F NMR Spectra

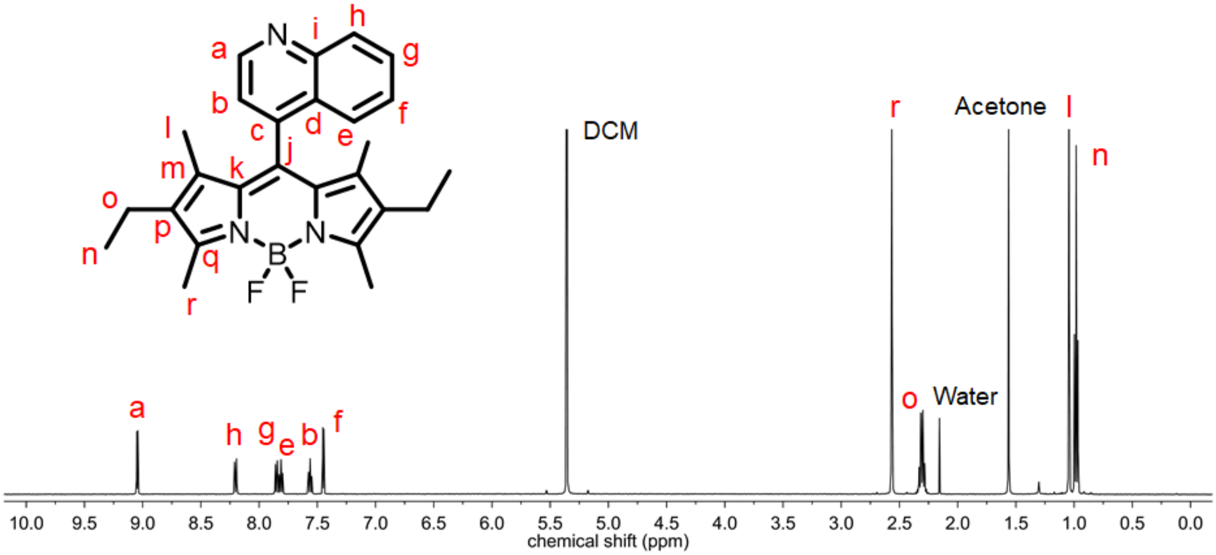

Figure S21. ^{1}H NMR of **BQu** (dichloromethane-*d*).

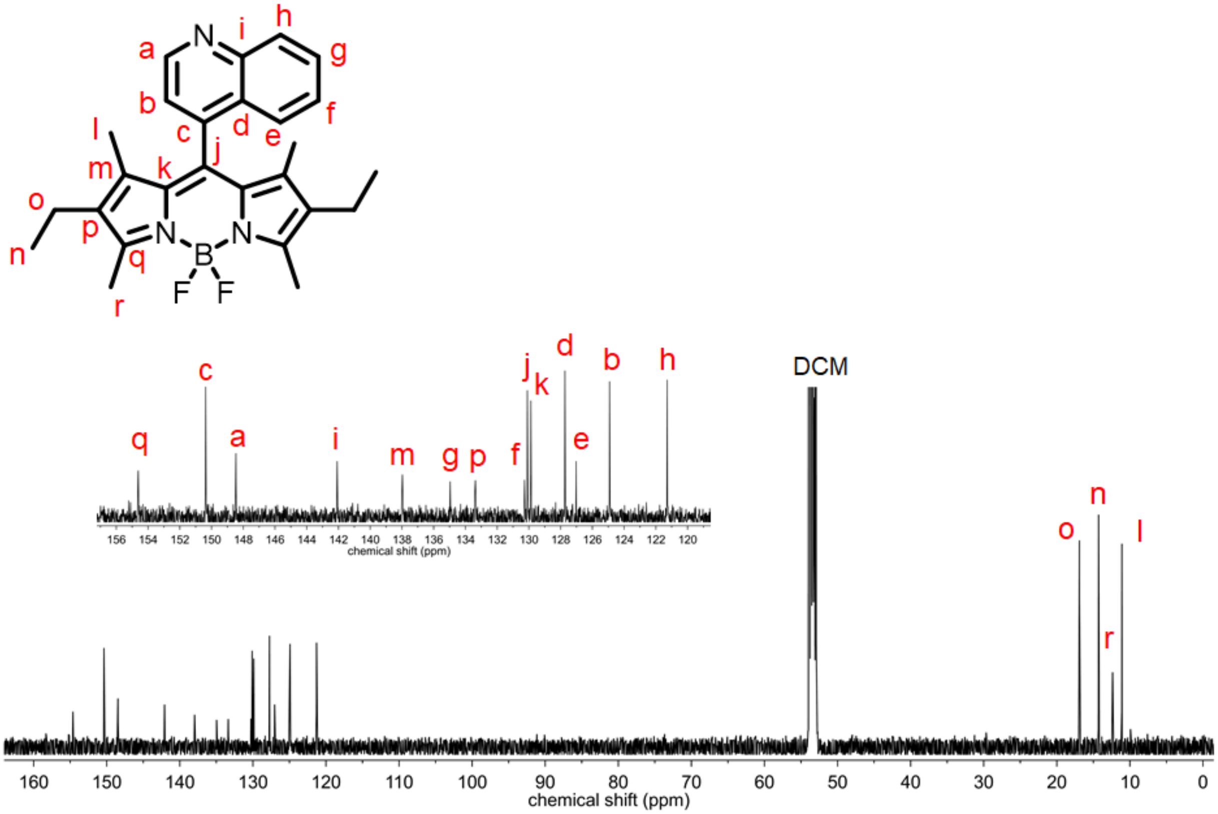

Figure S22. ^{13}C NMR of **BQu** (dichloromethane-*d*), with zoom.

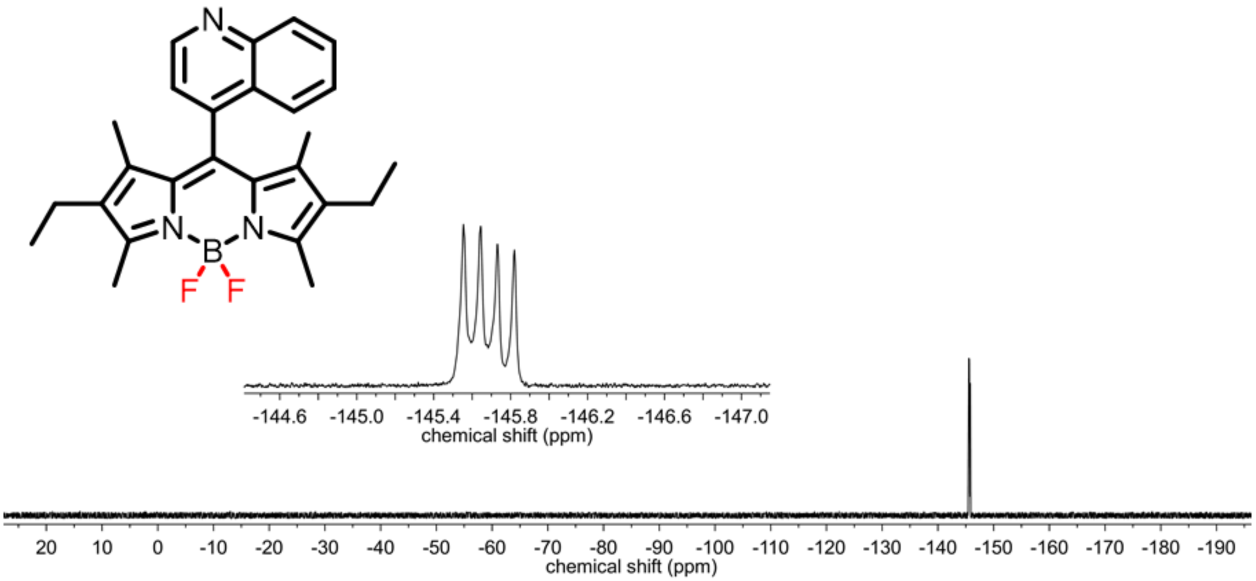

Figure S23. ^{19}F NMR of **BQu** (dichloromethane-*d*), with zoom.

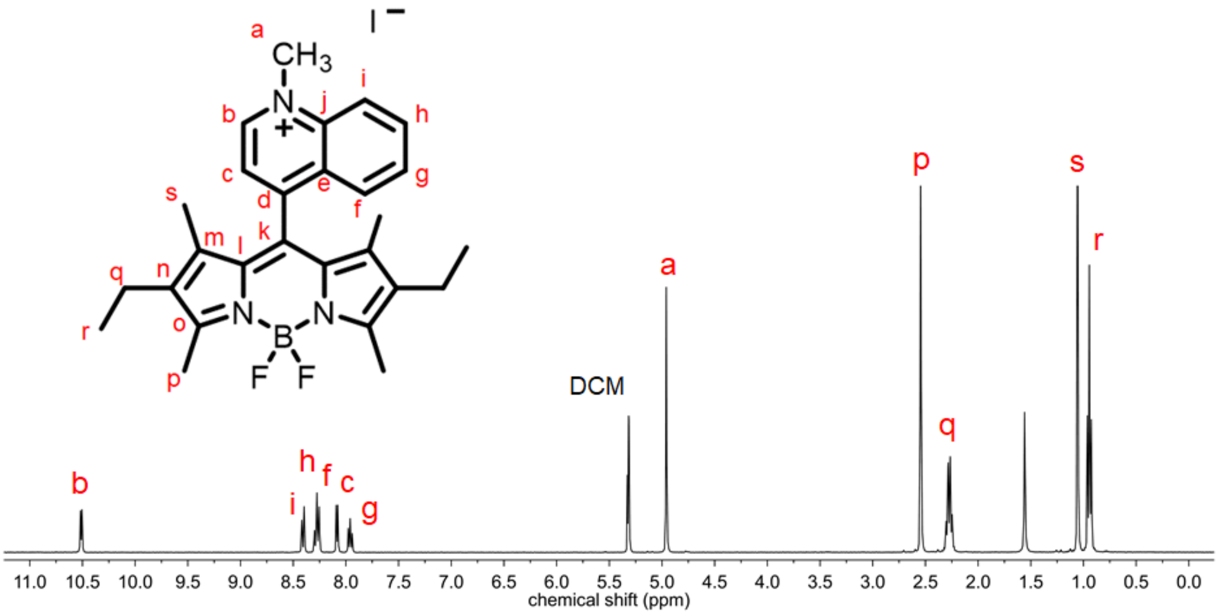

Figure S24. ^{1}H NMR of **BQuMe•**I (dichloromethane-*d*).

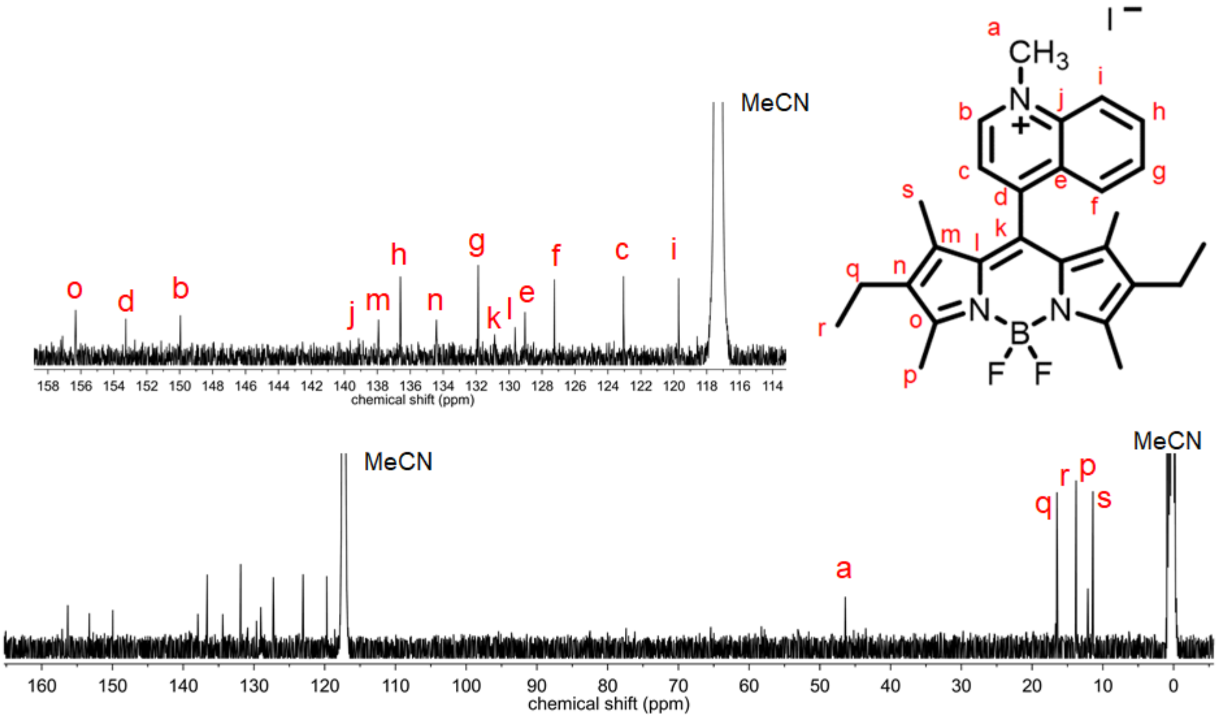

Figure S25. ^{13}C NMR of **BQuMe**•I (MeCN), with zoom.

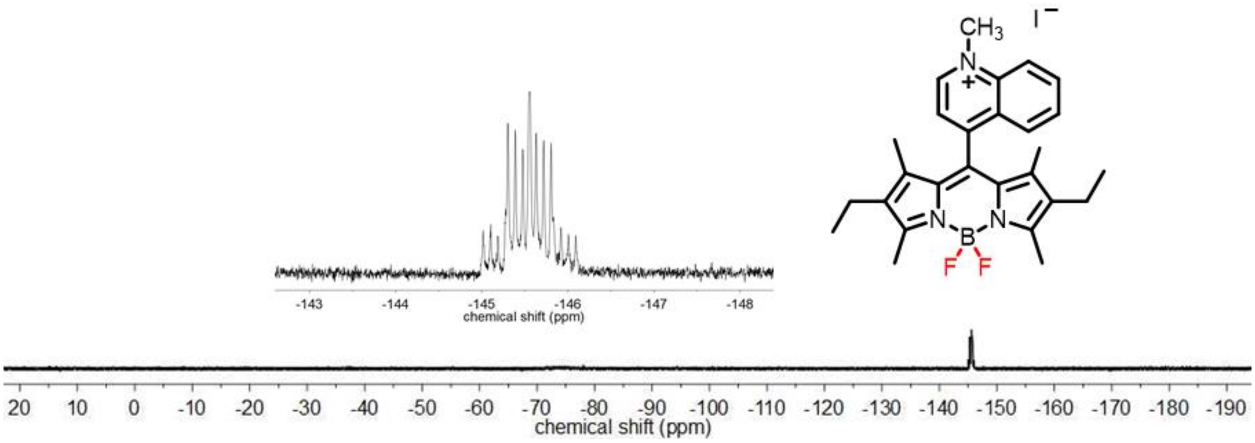

Figure S26. ^{19}F NMR of **BQuMe•**I (dichloromethane-*d*), with zoom.

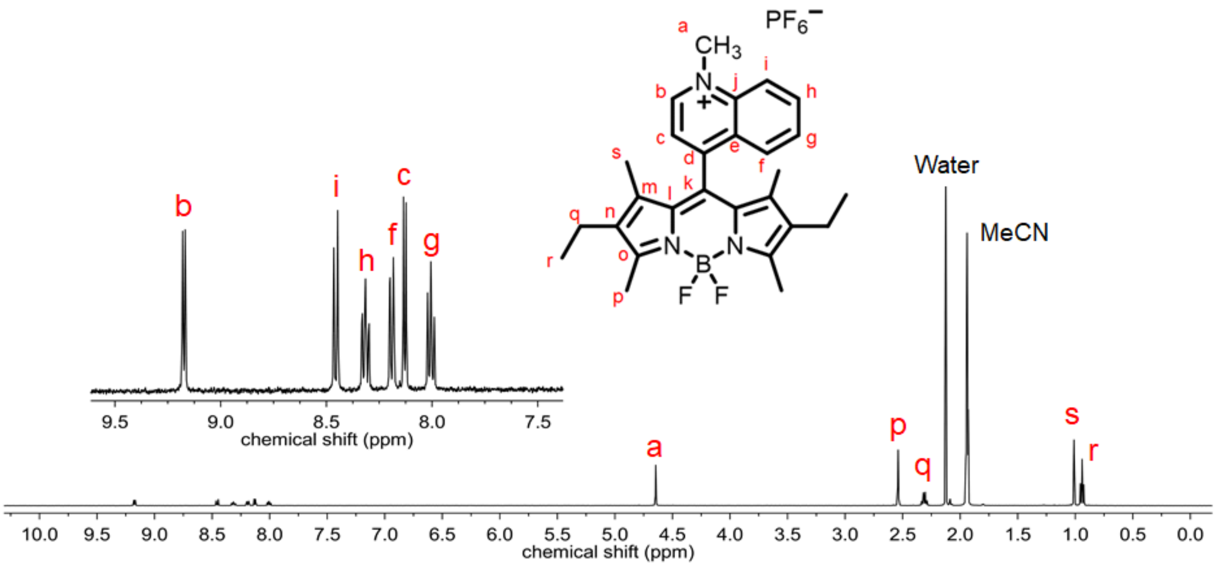

Figure S27. ^{1}H NMR of **BQuMe•**PF$_6$ (MeCN-*d*), with zoom.

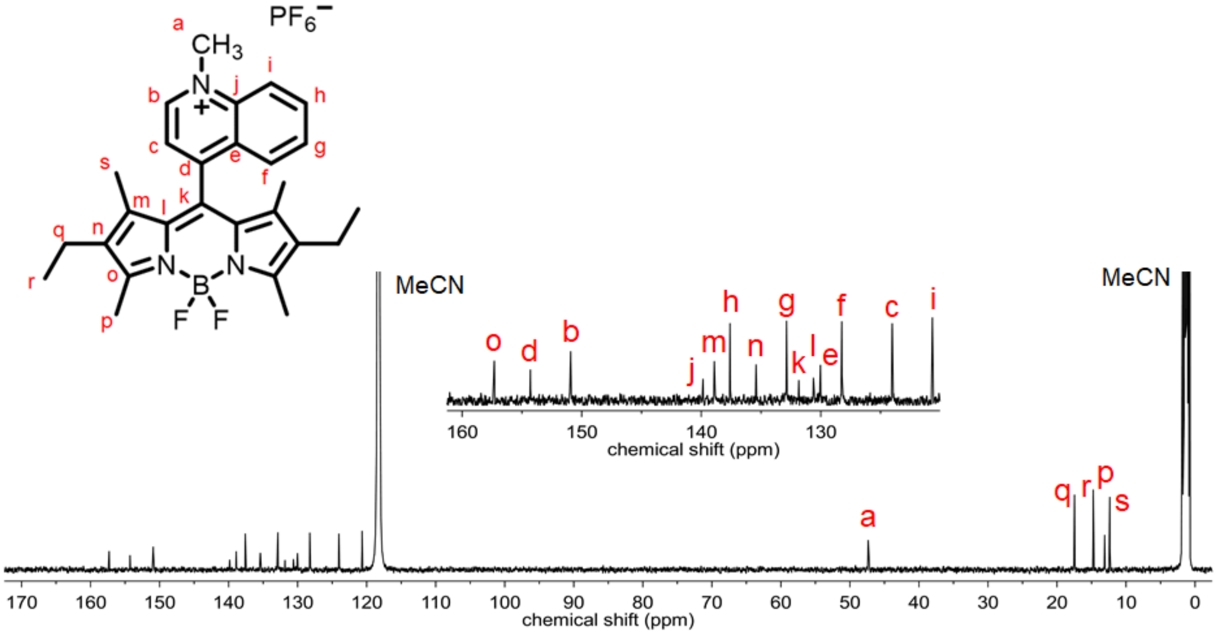

Figure S28. ^{13}C NMR of **BQuMe**•PF$_6$ (MeCN-*d*), with zoom.

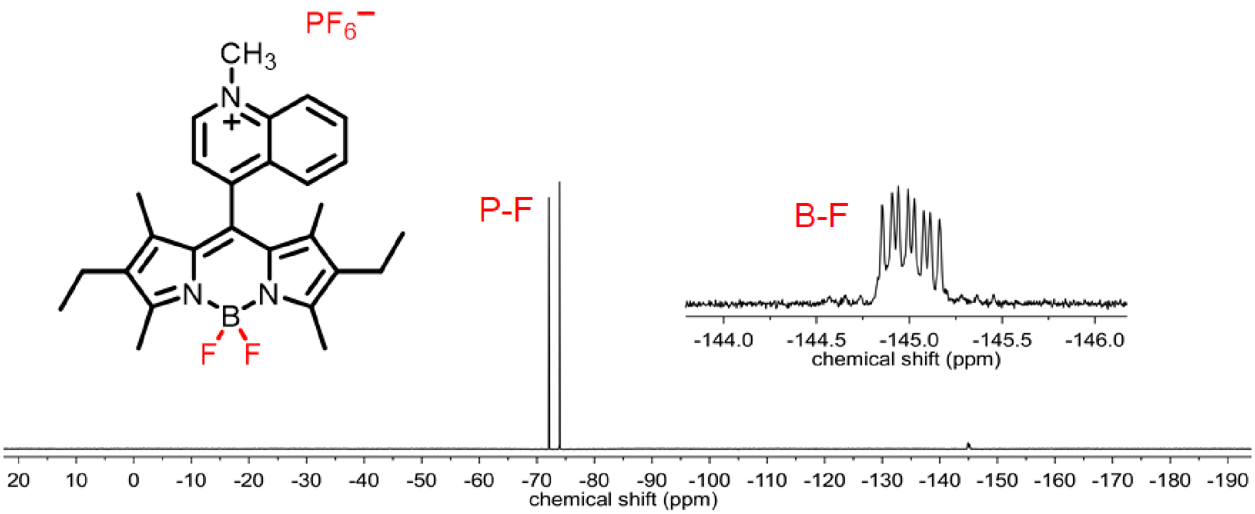

Figure S29. ^{19}F NMR of **BQuMe**•PF$_6$ (MeCN-*d*), with zoom.

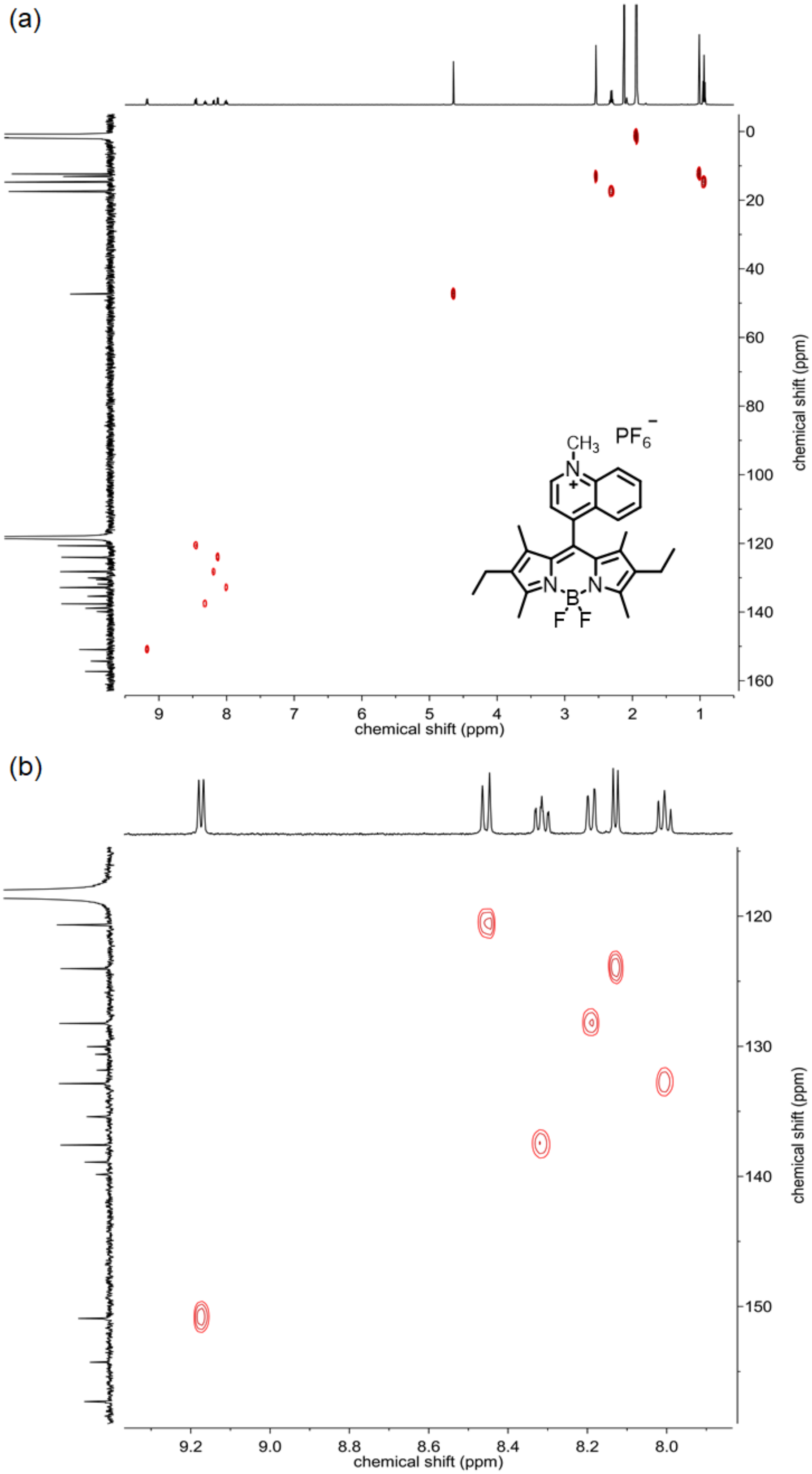

Figure S30. (a) HSQC NMR and (b) zoomed HSQC of **BQuMe**•PF_6 in MeCN-*d*.

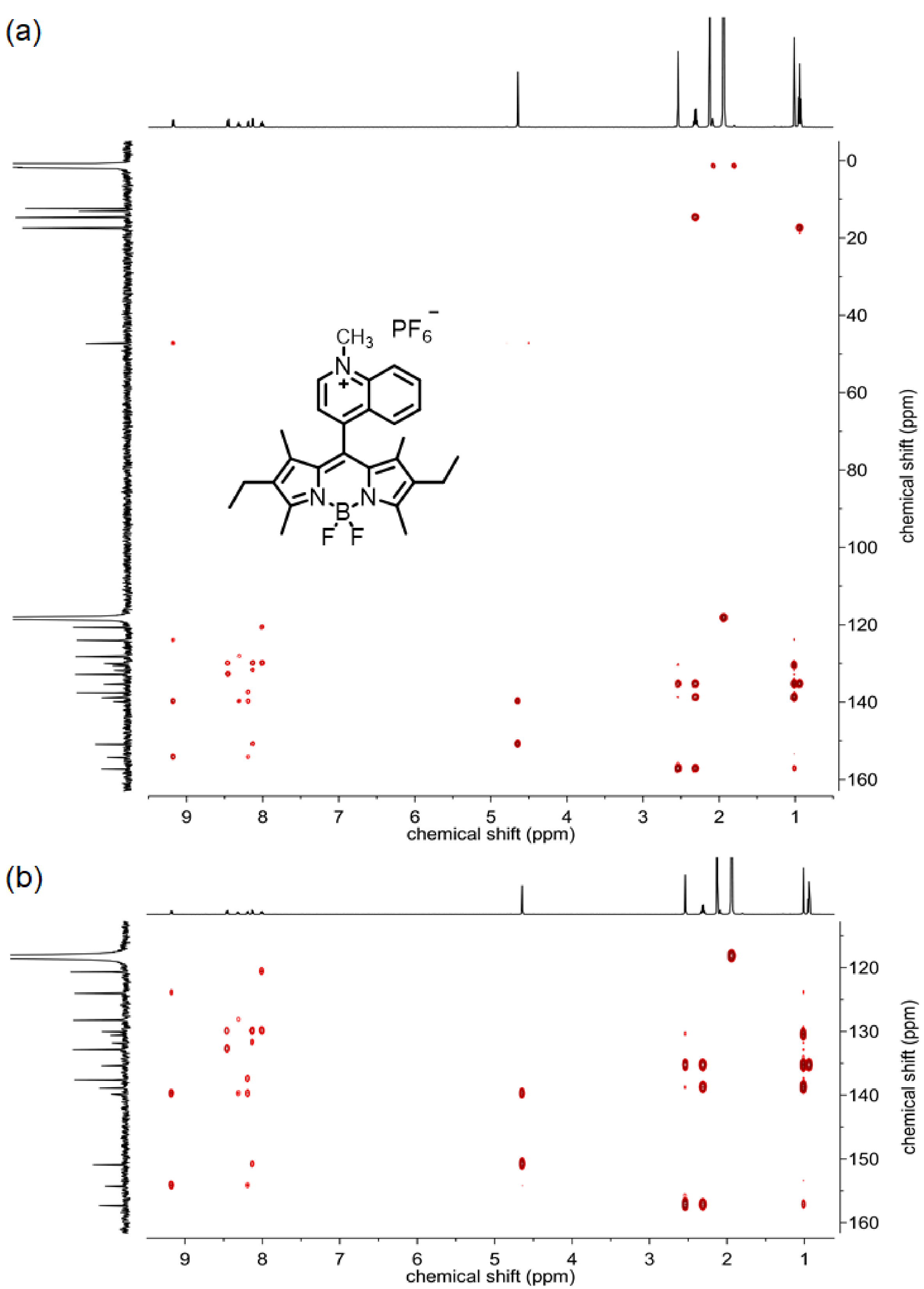

Figure S31. (a) HMBC NMR and (b) zoomed HMBC of **BQuMe**•PF_6 in MeCN-*d*.

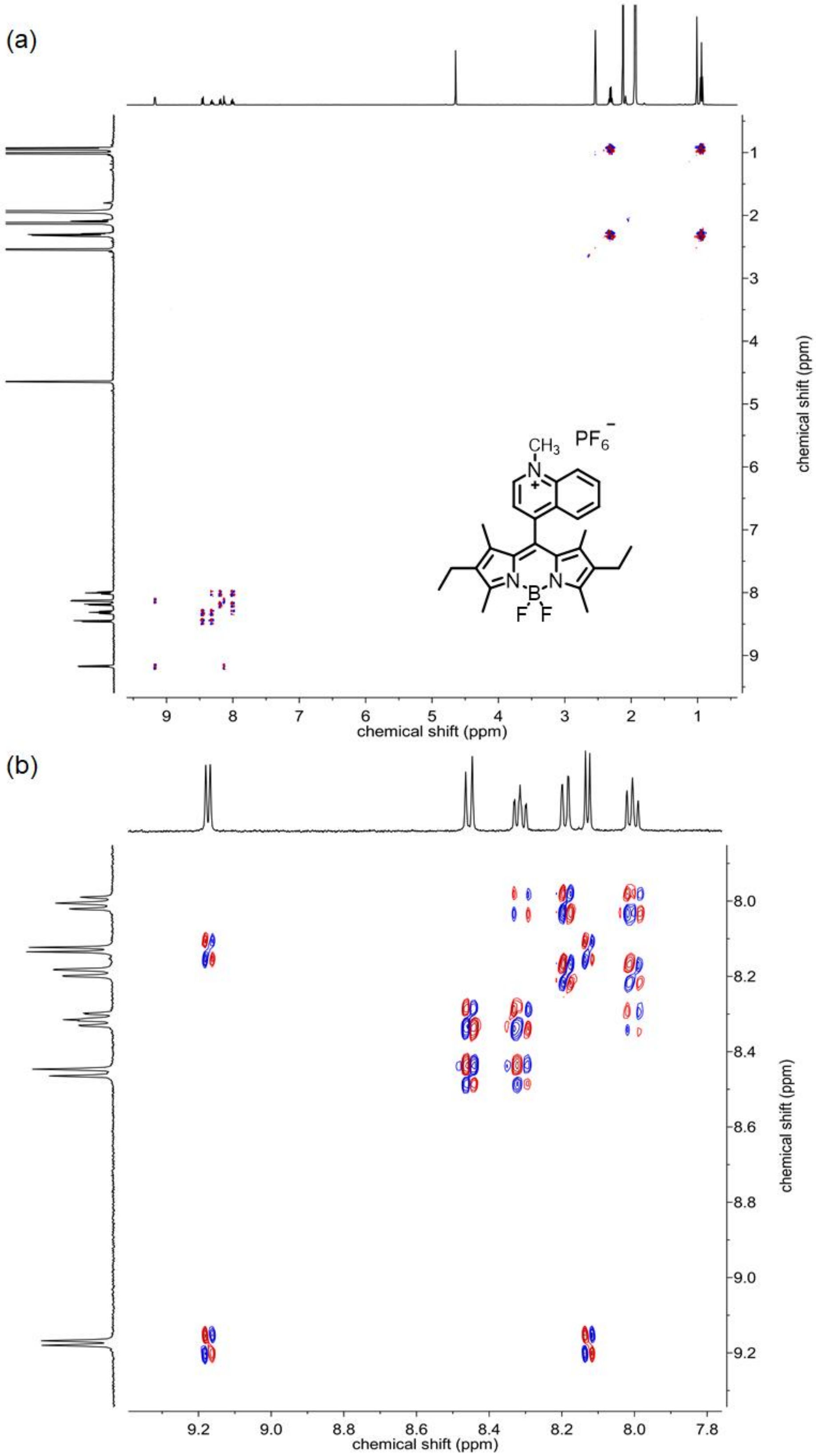

Figure S32. (a) DQCOSY NMR and (b) zoomed DQCOSY of **BQuMe**•PF_6 in MeCN-*d*.

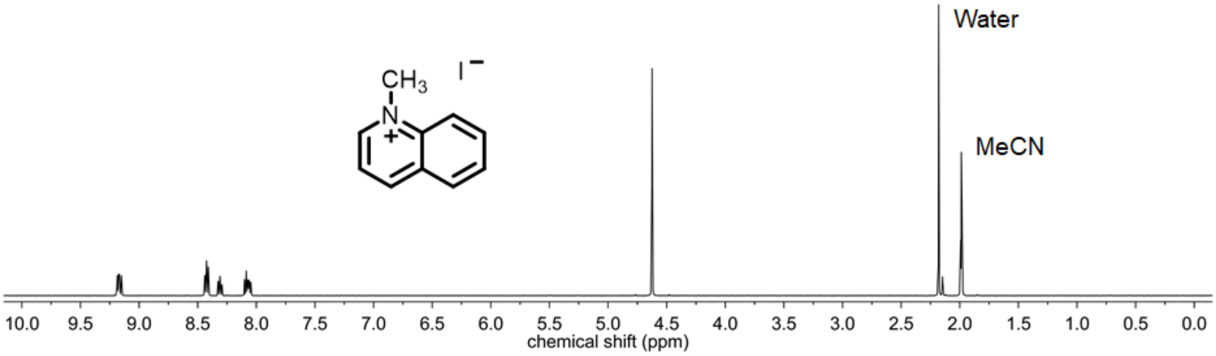

Figure S33. ^{1}H NMR of **QuMe•**I (MeCN-*d*).

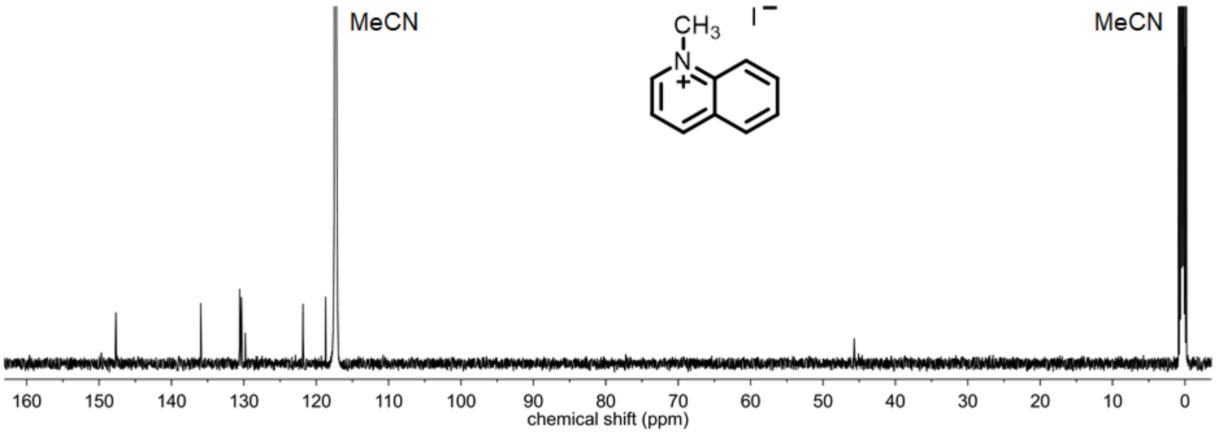

Figure S34. ^{13}C NMR of **QuMe•**I (MeCN-*d*).

S7. Coordinates of Computed Structures

xyz Optimized Coordinate of S_0 state

Molecule: **BQu**
Energy: -1396.89831048 a.u.
Charge: 0
Singlet State
No imaginary frequency

F	2.14328200	3.08818400	-0.76459600
F	1.65798100	2.86189600	1.46779300
N	-0.03202100	2.20011800	-0.13685400
N	2.04021600	0.84921000	0.15975700
N	-2.27363100	-3.79947400	-1.37572200
B	1.47301800	2.28279100	0.18857600
C	-0.90162700	3.23691100	-0.18232500
C	-2.19540000	2.75676800	-0.50942600
C	-2.10086900	1.36710100	-0.65751400
C	-0.73143400	1.02021700	-0.42312700
C	-0.06619700	-0.21217100	-0.42292100
C	1.29935100	-0.30516100	-0.12648400
C	2.18458100	-1.42745900	-0.04274600
C	3.44686000	-0.92077600	0.29253000
C	3.32264900	0.48775800	0.40123200
C	-0.49824400	4.64264200	0.11022200
H	-0.43916800	4.80822900	1.19238000
H	-1.23090600	5.34253500	-0.29522600
H	0.48291400	4.87063900	-0.31073500
C	-3.43299100	3.60208100	-0.61051100
H	-4.12356200	3.15904600	-1.33560100
H	-3.17294500	4.58937800	-1.00808600
C	-4.15171100	3.77247800	0.73971200
H	-5.04633100	4.39467800	0.63096700
H	-3.49292300	4.24687300	1.47472800
H	-4.45652200	2.80047400	1.14158300
C	-3.24086700	0.44969000	-0.98097800
H	-4.15955400	1.02136500	-1.12330300
H	-3.41863100	-0.27020100	-0.17620100
H	-3.05623000	-0.12717700	-1.89130700
C	-0.82912500	-1.45178500	-0.73944200
C	-1.49308800	-2.17584200	0.29261100
C	-1.47280400	-1.78061800	1.65669700
H	-0.92805500	-0.88636400	1.94012500
C	-2.13826500	-2.52346300	2.60776000
H	-2.11843000	-2.21447500	3.64784800

C	-2.85105000	-3.69187200	2.23663300
H	-3.37043200	-4.26609500	2.99724000
C	-2.88666600	-4.09992400	0.92072600
H	-3.42616600	-4.99135700	0.61792300
C	-2.21098100	-3.35603900	-0.08261300
C	-1.64150400	-3.09826100	-2.29872200
H	-1.70301100	-3.46750000	-3.31996700
C	-0.90636900	-1.91869500	-2.03263900
H	-0.41322700	-1.39408700	-2.84357100
C	1.86143500	-2.87399200	-0.26417900
H	1.56895300	-3.06847100	-1.30051500
H	1.03602800	-3.20979000	0.36955300
H	2.73084200	-3.49524400	-0.04163000
C	4.72467200	-1.69346800	0.45519600
H	4.50446700	-2.69039300	0.85116200
H	5.35726400	-1.20573400	1.20497500
C	5.51109400	-1.83031500	-0.86062700
H	6.43601000	-2.39613800	-0.70675900
H	5.77526800	-0.84563900	-1.26058600
H	4.91305400	-2.34942000	-1.61698400
C	4.39779600	1.47788700	0.69800400
H	5.25988100	0.98262400	1.14764500
H	4.04340200	2.25909300	1.37352400
H	4.73413200	1.96736300	-0.22351600

Molecule: **BQuMe$^+$**
Energy: -1436.65998741 a.u.
Charge: +1
Singlet State
No imaginary frequency

F	3.92229800	0.23633600	-0.90675700
F	3.55406200	0.49009100	1.34493100
N	1.92108700	1.41410300	-0.18633500
N	2.13918300	-1.05198200	0.10989300
N	-4.20403700	-0.49300700	-1.06759700
B	2.92604600	0.27645700	0.09601700
C	2.20368300	2.73597100	-0.24918400
C	1.01383200	3.46456400	-0.51274200
C	-0.03176800	2.53960700	-0.60102500
C	0.54712500	1.24427100	-0.39675900
C	-0.01095800	-0.03842800	-0.36215900
C	0.76161700	-1.17723900	-0.10806000
C	0.42392900	-2.56718200	-0.01291300

C	1.61284900	-3.25056600	0.26368300
C	2.65249300	-2.28546800	0.32477300
C	3.57391600	3.28090000	-0.03149300
H	3.78392300	3.37026300	1.04092800
H	3.66350700	4.27523800	-0.47234000
H	4.33516700	2.62899900	-0.46351600
C	0.91985700	4.96025400	-0.61135600
H	0.10631300	5.23442700	-1.29070900
H	1.83547100	5.35652800	-1.06385300
C	0.69529600	5.63454800	0.75387000
H	0.63472100	6.72251100	0.64619900
H	1.51521700	5.40451200	1.44222500
H	-0.23508400	5.28247800	1.21162300
C	-1.47010200	2.87786600	-0.85265100
H	-1.59530600	3.95840500	-0.93693000
H	-2.11787200	2.53647100	-0.03978600
H	-1.84154800	2.42724100	-1.77774200
C	-1.47316800	-0.19499500	-0.59564400
C	-2.38331900	-0.16095000	0.49591800
C	-1.94955300	0.02160300	1.83478800
H	-0.89011900	0.13907000	2.02818900
C	-2.85971600	0.04868400	2.86667400
H	-2.52178400	0.18871500	3.88719100
C	-4.23881800	-0.10616200	2.59873700
H	-4.95031000	-0.08392200	3.41678600
C	-4.70087300	-0.28591100	1.30982500
H	-5.76074700	-0.40147100	1.13308100
C	-3.78029900	-0.31538000	0.24153000
C	-3.33142900	-0.52004300	-2.07955400
H	-3.74330300	-0.66150000	-3.06977300
C	-1.95995400	-0.37399300	-1.87606700
H	-1.29723000	-0.40410900	-2.73114500
C	-5.64469200	-0.65577000	-1.35754700
H	-5.76749400	-0.78555800	-2.42945600
H	-6.18236300	0.23563800	-1.03316900
H	-6.02150500	-1.53653300	-0.83715100
C	-0.92395200	-3.20165400	-0.17758500
H	-1.32895200	-3.04052000	-1.18112700
H	-1.65372600	-2.80892200	0.53642200
H	-0.85676600	-4.27918500	-0.02032400
C	1.80139600	-4.73275300	0.41576000
H	0.88976200	-5.18028800	0.82448700
H	2.58841300	-4.92901300	1.15225100
C	2.16199200	-5.42686900	-0.90972100
H	2.29557300	-6.50360600	-0.76234100
H	3.09139800	-5.02074500	-1.32246500

H	1.37179100	-5.27729600	-1.65287900
C	4.10545800	-2.52747300	0.55288500
H	4.26099500	-3.49856500	1.02562900
H	4.54455700	-1.75004500	1.18077600
H	4.64715000	-2.52774700	-0.40034800

xyz Optimized Coordinate of S_1 state

Molecule: **BQu**
Energy: -1396.80885154 a.u.
Charge: 0
Singlet State

F	2.39640800	2.90971000	-0.83610100
F	2.06404100	2.69667500	1.42153900
N	0.23129100	2.13133700	-0.06595800
N	2.22392600	0.67350000	0.09283100
N	-2.44860200	-3.74400700	-1.22690800
B	1.75028800	2.13207300	0.15875700
C	-0.54443600	3.23693400	-0.17619500
C	-1.85691300	2.84941100	-0.59187200
C	-1.86026800	1.45419900	-0.74560300
C	-0.55253100	0.99957200	-0.38473000
C	0.00551600	-0.30705600	-0.32580000
C	1.38557300	-0.45532000	-0.04140400
C	2.18204300	-1.62641700	0.18161900
C	3.49423600	-1.18345200	0.40161300
C	3.48451500	0.24515900	0.34577200
C	-0.02759900	4.60731700	0.06964800
H	0.48538000	4.66450600	1.03564400
H	-0.83849500	5.33570100	0.05454100
H	0.70958500	4.88936600	-0.69338100
C	-3.01523800	3.77309900	-0.79685200
H	-3.57949400	3.45969600	-1.68285100
H	-2.65553300	4.78579400	-1.00282100
C	-3.96709700	3.80583500	0.41714600
H	-4.80840600	4.47970300	0.22575500
H	-3.44271900	4.15433100	1.31248900
H	-4.36534600	2.80793100	0.62524400
C	-3.02538100	0.64483200	-1.22178800
H	-3.72948000	1.28311600	-1.76119600
H	-3.57049500	0.17848500	-0.39286000
H	-2.71262000	-0.15915700	-1.89151400
C	-0.82503200	-1.49059200	-0.59874200
C	-1.88698100	-1.88208400	0.28132400

C	-2.16157000	-1.22506500	1.50779600
H	-1.54150700	-0.38685200	1.80695500
C	-3.20297600	-1.63836800	2.31512100
H	-3.40032900	-1.12407500	3.25028500
C	-4.01201800	-2.73310200	1.92931400
H	-4.83259100	-3.04712700	2.56690000
C	-3.75315800	-3.40867400	0.75335200
H	-4.35396800	-4.25919700	0.44722000
C	-2.68140900	-3.01480000	-0.09051700
C	-1.42905000	-3.37366600	-1.99185300
H	-1.25700200	-3.96473200	-2.88908200
C	-0.59590900	-2.27189800	-1.72497700
H	0.19872100	-2.01748400	-2.41780300
C	1.73140400	-3.05200700	0.23221000
H	1.60315100	-3.48622000	-0.76658200
H	0.77115800	-3.15264000	0.74427600
H	2.46804300	-3.65928300	0.76391200
C	4.69988500	-2.03803900	0.63675900
H	4.43278200	-2.87200000	1.29602800
H	5.46858600	-1.46443200	1.16340400
C	5.29055600	-2.60315800	-0.67146000
H	6.16174100	-3.23108700	-0.45855900
H	5.60392900	-1.79360600	-1.33831400
H	4.54986300	-3.21015200	-1.20137500
C	4.61845400	1.17897300	0.56634900
H	5.56519300	0.63929000	0.59586200
H	4.49794000	1.72216100	1.51280300
H	4.66243100	1.93453100	-0.22484500

Molecule: **BQuMe**$^+$
Energy: -1436.59945560 a.u.
Charge: +1
Singlet State

F	-3.92744900	0.41004700	0.94094700
F	-3.59167000	0.60086300	-1.32139300
N	-1.89606300	1.47964400	0.17027100
N	-2.22300800	-0.97083700	-0.09401800
N	4.17872900	-0.68597800	1.08349900
B	-2.97177200	0.38919700	-0.08318600
C	-2.10791200	2.80014100	0.24614100
C	-0.85883600	3.48276900	0.51676000
C	0.12520700	2.52094400	0.60426200
C	-0.52832300	1.24059000	0.38978100

C	-0.00082700	-0.05587600	0.36530400
C	-0.84334400	-1.14421700	0.10994500
C	-0.54252300	-2.56071700	-0.01645200
C	-1.73727200	-3.19223900	-0.28951500
C	-2.76678500	-2.17306400	-0.32486700
C	-3.43423300	3.44046600	0.10350400
H	-3.36568700	4.28606500	-0.58774900
H	-3.73908000	3.85136300	1.07428500
H	-4.19706400	2.74703500	-0.24214600
C	-0.71831100	4.96959600	0.61855000
H	0.06681400	5.21163000	1.34078900
H	-1.64511800	5.39837000	1.01243900
C	-0.38475000	5.61876200	-0.73947100
H	-0.29751900	6.70345700	-0.62892100
H	-1.16441100	5.41200100	-1.47919400
H	0.56178500	5.23365200	-1.13044300
C	1.57763000	2.76636700	0.85088000
H	1.75477000	3.82748500	1.03120100
H	2.17775200	2.46184400	-0.01173500
H	1.94089600	2.19932900	1.71095200
C	1.44892500	-0.27473400	0.59256800
C	2.37674100	-0.21719900	-0.49610400
C	1.98815900	0.03780600	-1.82986300
H	0.93843700	0.19791200	-2.04927400
C	2.92148700	0.08803100	-2.86403100
H	2.59109200	0.28698400	-3.87817300
C	4.27410400	-0.11742300	-2.59016200
H	5.00917300	-0.08017400	-3.38677800
C	4.69540100	-0.37461600	-1.27976000
H	5.74814800	-0.53187600	-1.08740400
C	3.76850800	-0.42821300	-0.23112600
C	3.26225600	-0.73887300	2.11326500
H	3.66467500	-0.94323200	3.09475600
C	1.92531700	-0.54091900	1.89020300
H	1.24321500	-0.59084500	2.73042300
C	5.59268900	-0.90319800	1.37297100
H	5.70798400	-1.08724700	2.43958400
H	6.18215100	-0.02275900	1.10060000
H	5.97060700	-1.76956600	0.82217500
C	0.79292400	-3.21753600	0.11004200
H	1.21400400	-3.07273900	1.10833300
H	1.50891200	-2.80131100	-0.60352200
H	0.70385900	-4.28912100	-0.07326200
C	-1.99496200	-4.65494900	-0.47694000
H	-1.13590900	-5.11343200	-0.97545400
H	-2.85063400	-4.79237100	-1.14537800

C	-2.26037500	-5.37830000	0.85827200
H	-2.45112400	-6.44072000	0.68147900
H	-3.12964800	-4.95546400	1.37144000
H	-1.39795900	-5.28796800	1.52547000
C	-4.20326500	-2.39615400	-0.60069200
H	-4.32789000	-2.65073500	-1.66103300
H	-4.80993800	-1.52169300	-0.37704000
H	-4.56473500	-3.25333200	-0.02552200

S8. References

S1. Rohwer, L. S.; Martin, J. E., *J. Lumin.* **2005,** *115*, 77-90.

S2. Suzuki, K.; Kobayashi, A.; Kaneko, S.; Takehira, K.; Yoshihara, T.; Ishida, H.; Shiina, Y.; Oishi, S.; Tobita, S., *Phys. Chem. Chem. Phys.* **2009,** *11*, 9850-9860.

S3. Lakowicz, J. R., *Topics in fluorescence spectroscopy*. Plenum Press: New York, 1994; Vol. 4.

S4. SAINT, B. A. X.-R. S., Madison, WI, current version.

S5. SADABS, B. A. X.-R. S., Madison, WI, current version.

S6. Sheldrick, G. M., *Acta. Crystallogr.* **2008,** *A64*, 112-122.

S7. Frisch, M. J.; Trucks, G. W.; Schlegel, H. B.; Scuseria, G. E.; Robb, M. A.; Cheeseman, J. R.; Scalmani, G.; Barone, V.; Petersson, G. A.; Nakatsuji, H.; Li, X.; Caricato, M.; Marenich, A. V.; Bloino, J.; Janesko, B. G.; Gomperts, R.; Mennucci, B.; Hratchian, H. P.; Ortiz, J. V.; Izmaylov, A. F.; Sonnenberg, J. L.; Williams; Ding, F.; Lipparini, F.; Egidi, F.; Goings, J.; Peng, B.; Petrone, A.; Henderson, T.; Ranasinghe, D.; Zakrzewski, V. G.; Gao, J.; Rega, N.; Zheng, G.; Liang, W.; Hada, M.; Ehara, M.; Toyota, K.; Fukuda, R.; Hasegawa, J.; Ishida, M.; Nakajima, T.; Honda, Y.; Kitao, O.; Nakai, H.; Vreven, T.; Throssell, K.; Montgomery Jr., J. A.; Peralta, J. E.; Ogliaro, F.; Bearpark, M. J.; Heyd, J. J.; Brothers, E. N.; Kudin, K. N.; Staroverov, V. N.; Keith, T. A.; Kobayashi, R.; Normand, J.; Raghavachari, K.; Rendell, A. P.; Burant, J. C.; Iyengar, S. S.; Tomasi, J.; Cossi, M.; Millam, J. M.; Klene, M.; Adamo, C.; Cammi, R.; Ochterski, J. W.; Martin, R. L.; Morokuma, K.; Farkas, O.; Foresman, J. B.; Fox, D. J. *Gaussian 16 Rev. A.03*, Wallingford, CT, 2016.

S8. Cossi, M.; Rega, N.; Scalmani, G.; Barone, V., *J. Comput. Chem.* **2003,** *24*, 669-681.